



UNIVERSITY *of the*
WESTERN CAPE

**EVALUATING THE SPECIFICITY OF CANCER CELL TARGETING
PEPTIDES FOR APPLICATIONS IN CANCER DIAGNOSTICS**



MARGARET KENA MAZYAMBE
UNIVERSITY of the
WESTERN CAPE

A thesis submitted in partial fulfillment of the requirements for the degree of
Magister Scientiae in the Department of Biotechnology, University of Western Cape

Supervisor: Dr Mervin Meyer

May 2013



UNIVERSITY *of the*
WESTERN CAPE

ABSTRACT

EVALUATING THE SPECIFICITY OF CANCER CELL TARGETING PEPTIDES FOR APPLICATIONS IN CANCER DIAGNOSTICS.

M. K. Mazyambe,

M.Sc thesis, Department of Biotechnology, Faculty of Science University of Western Cape

South Africa

Cancer is a disease most often associated with poor prognosis. During the development of the disease, cells acquire genetic mutations which result in changes in bio-molecules (DNA and protein), thus altering normal functioning of cells. These bio-molecules can thus serve as biomarkers for the diagnosis of cancer and can also facilitate the early detection of cancer. Antibodies labelled with organic fluorophores are typically used in immunohistochemistry techniques to screen cancerous tissue for the presence of biomarkers. More recently, researchers started to use cancer specific peptides (e.g LYP-1, RGD,) rather than antibodies for this purpose. Advantages of peptides include high affinity to their binding target, rapid accumulation at target sites and the ability to evade the immune system. Fluorescent nanocrystals or quantum dots are emerging as nanoparticles that can replace organic fluorophores. Several properties of quantum dots make these nanoparticles an ideal application in the detection of cancer related biomarkers. These include size tunable fluorescence emission, resistance to photobleaching as well as high quantum yields that result in bright emission of fluorescence. The aim of this research project was to investigate the specific binding of selected peptides to cancer cells using functionalized quantum dots. Since the cost of synthetic peptides are so high, the aim of this study was also to express

these peptides in *E.coli* bacterial cells. Cancer targeting peptides were identified from literature and oligonucleotides with sequences encoding these peptides were designed. Four oligonucleotides encoding the peptides p6.1, p.L, MV and NL1.1 were successfully cloned using the pET21b plasmid vector. However, the peptides were not successfully expressed in *E.coli*. Cancer targeting peptides namely p.C, p.H, p.L, p6.1 and Frop-1 were chemically synthesized and obtained from GL biochem (Shanghai). These peptides were conjugated to quantum dots (Qdot 525) using 1-ethyl-3-(3-dimethylamino) carbodiimide HCl (EDC) chemistry. The peptide-quantum dot conjugates were applied to cancer cells to achieve specific binding. The Kmst-6 non-cancerous cell line served as a control. The binding of the peptide-quantum dot conjugates was analyzed using flow cytometry and fluorescence microscopy. The p.H peptide revealed the highest binding affinity to cancer cells as indicated by fluorescence intensity. This was followed by the p.C peptide which showed differential binding amongst the cancer cell lines. The Frop-1 peptide displayed the lowest binding affinity, while the binding affinity of the peptides to Kmst-6 cell lines was very low. This study demonstrated that the cancer targeting peptides used in this study bind to cancer cells and that the specificity with which these peptides bind to the cells depends on the cell types and the peptide

KEYWORDS:

Antibodies

Binding

Bioconjugation

Cancer targeting peptides

Cell surface proteins

Diagnosis

Flow cytometry

Microscopy

Nanotechnology

Quantum dots



The logo of the University of the Western Cape, featuring a classical building facade with columns and a pediment, with the text 'UNIVERSITY of the WESTERN CAPE' below it.

DEDICATION

For my parents (Langson and Monica), husband (Aubrey) sisters and brother (Melanie, Miria, Mushinka) and my daughter (Mambo)

DECLARATION

I declare that “**Evaluating the Specificity of Cancer Cell Targeting Peptides for Applications in Cancer Diagnostics**” is my own work that has not been submitted for any degree or examination in any other university and that all the sources I have used or quoted have been indicated and acknowledged by complete references.




MARGARET KENA MAZYAMBE

Signed.....

May 2013

TABLE OF CONTENTS

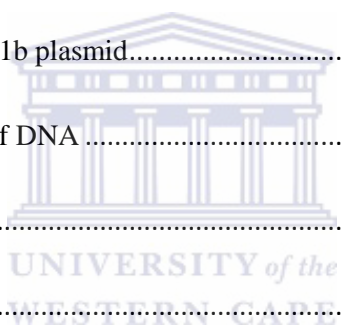
PAGE

ABSTRACT.....	I
KEYWORDS:.....	III
DEDICATION	IV
DECLARATION	V
LIST OF TABLES	XII
LIST OF FIGURES	XIII
ABBREVIATIONS	XV
ACKNOWLEDGEMENTS	XIX
 UNIVERSITY of the WESTERN CAPE	
CHAPTER 1: INTRODUCTION	1
1.1. Background.....	1
1.2. Molecular biology of cancer	2
1.2.1. Genetic changes	2
1.2.1.1. Oncogenes.....	5
1.2.1.1.1. Growth factor and Growth factor receptors	6
1.2.1.1.2. Serine/threonine kinases	7
1.2.1.1.3. Transcription factors	7
1.2.1.2. Tumor suppressor genes.....	8

1.2.2. Epigenetic changes.....	9
1.3. Distinguishing characteristics of cancer	10
1.3.1. Cell cycle deregulation	11
1.3.2. Apoptosis evasion	13
1.3.2.1. The intrinsic or mitochondrial pathway	13
1.3.2.2. Extrinsic pathway or the death receptor pathway	14
1.3.3. Cell immortality	16
1.3.4. Metastasis.....	16
1.4. Cancer diagnosis	18
1.5. Cancer biomarkers	19
1.6. Cancer targeting peptides.....	20
1.7.1 Quantum dots	23
1.7.1.1. Properties of quantum dots	25
1.7.1.2. Bioconjugation of quantum dots	27
1.8. Tumour targeting using quantum dots and peptides for Cancer Diagnosis	29
1.9. Objectives	31



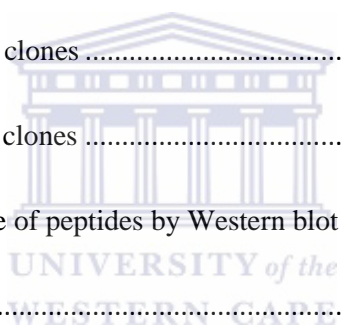
CHAPTER 2: MATERIALS AND METHODS	32
2.1 Materials used and Suppliers	32
2.1.1. List of kits	35
2.2. Solutions and Buffers.....	35
2.3. Design of oligonucleotides for the expression of peptides	37
2.3.2 Cloning vector.....	39
2.4. Preparation of pET21b DNA	41
2.4.1. Preparation of pET21b plasmid using cesium chloride/ethidium bromide fractionation	41
2.4.2. Restriction digestion of pET21b plasmid.....	42
2.4.3. Agarose gel electrophoresis of DNA	44
2.4.4. Gel purification of DNA	44
2.5. Strains	46
2.6. Preparation of competent <i>E. coli</i> cells	46
2.7. Cloning of oligonucleotides	47
2.7.1. Annealing of oligonucleotides	47
2.7.2. Ligation of oligonucleotides into pET21b plasmid.....	47
2.7.3. Transformation.....	52
2.7.4. Screening of positive colonies	52
2.8. Protein expression.....	52
2.8.1. Protein precipitation.....	53



2.9. 1D SDS-Polyacrylamide Gel Electrophoresis	54
2.9.1. Gel preparation.....	54
2.9.2 Sample preparation and gel loading.....	56
2.9.3. Gel staining	56
2.10. Western blot.....	56
2.10.1 Blot transfer of proteins onto PVDF membrane	56
2.10.2 Western plot analysis of peptides.....	57
2.10.3. Development of the film.	57
2.11. Cell culture.....	58
2.11.1. Cell lines	58
2.11.2. Cell propagation.....	58
2.11.3 Trypsinization	58
2.12. Peptide design.....	59
2.13. Qdot 525 carboxyl nanocrystal conjugation	59
2.13.1. Conjugated nanocrystal purification	60
2.14. Cell staining	61
2.14.1. Preparation of cells for analysis by fluorescence microscopy	61
2.14.2. Microscopy analysis.....	61
2.14.3 Preparation of cells for Flow cytometry analysis.....	62
2.14.4. Flow cytometry analysis	62



2.14.4.1. Flow Cytometry Acquisition.....	62
CHAPTER 3: RESULTS	64
3.1. Cloning oligonucleotides into an expression vector	64
3.1.1. Introduction.....	64
3.1.2. Preparation of pET21b plasmid DNA.....	66
3.1.3. Restriction digestion of pET21b plasmid DNA	67
3.1.4. Ligation of oligonucleotides encoding peptides into pET21b plasmid.....	68
3.1.5. Screening for positive clones	69
3.1.6. Sequence analysis of positive clones	69
3.2.2. Expression screen of positive clones	71
3.2.2.1 Screening for the presence of peptides by Western blot analysis	73
3.4. Discussion.....	78
3.5. Limitations and recommendations	80
CHAPTER 4	82
4.1. Conjugation of cancer specific peptides to quantum dots.....	82
4.1.1. Introduction.....	82
4.1.2. Quantification of the binding of peptide-quantum dot conjugates to cells using flow cytometry and fluorescence microscopy	83
4.2. Summary	91



4.3. Discussion	92
4.3.1. Conclusion	97
4.4. Future Directions	98
4.4.1. Limitations of the study	98
References.....	99



LIST OF TABLES**PAGE**

Table 2.1: Peptide sequences and oligonucleotide sequences.....	38
Table 2.2: Reagents used to digest pET21b Plasmid using <i>XhoI</i>	43
Table 2.3: Reagents used to digest pET21b Plasmid using <i>NdeI</i>	43
Table 2.4: Bacterial strains used.....	46
Table 2.5: Reagents utilized in the ligation reactions of oligonucleotide encoding p.L.....	48
Table 2.6: Reagents utilized in the ligation reactions of oligonucleotide encoding p6.1.....	49
Table 2.7: Reagents utilized in the ligation reactions of oligonucleotide encoding MV.....	50
Table 2.8: Reagents utilized in the ligation reactions of oligonucleotide encoding NL1.1.....	51
Table 2.9: Stock solutions for the 18% separating gel solution.....	54
Table 2.10: Stock solutions for the 4% stacking gel solution.....	55
Table 2.11: Sequences of chemically synthesized peptides.....	59
Table 2.12: Reagents utilized for biomolecule conjugation to Qdot 525.....	60
Table 3.1: Number of colonies obtained following transformation of <i>E. coli</i> cells with pET21b containing oligonucleotides.....	68

LIST OF FIGURES	PAGE
Figure 1.1: Tumorigenesis development model.....	3
Figure 1.2: The cell cycle showing the M, G1, G2 and the S phase.....	11
Figure 1.3: The Extrinsic and intrinsic pathway involved in apoptosis.....	14
Figure 1.4: Structure of a quantum dot. The core of the quantum dot is made from group II and VI elements such as CdSe while the shell is made from ZnS.....	24
Figure 1.5: Quantum dot size and wave length.	25
Figure 1.6: Amide bond formation using EDC chemistry.....	29
Figure 2.1: Map of pET21 (+) plasmid.....	40
Figure 3.1: Cloning strategy for p6.1 peptide.....	65
Figure 3.2: Gel electrophoresis of pET21b plasmid.....	66
Figure 3.3: Agarose gel electrophoresis restriction digestion of pET21b.....	67
Figure 3.4: Translation of DNA sequences into protein sequences.....	70
Figure 3.5: SDS PAGE analysis of bacterial lysate.....	72
Figure 3.6: Western blot analysis of bacterial lysate.....	74
Figure 3.7: SDS PAGE analysis of precipitated protein secreted in culture medium.....	76
Figure 3.8: Western blot analysis of precipitated protein secreted in culture medium.....	77

Figure 4.1: Targeted binding of peptide conjugated quantum dots 525 to cancer cells.....85

Figure 4.2: Binding of p.C-Qdot 525 conjugate to cancer cells.....86

Figure 4.3: Binding of Frop-1-Qdot 525 conjugate to cancer cells.....87

Figure 4.4: Binding of p.H-Qdot 525 conjugate to cancer cells.....88

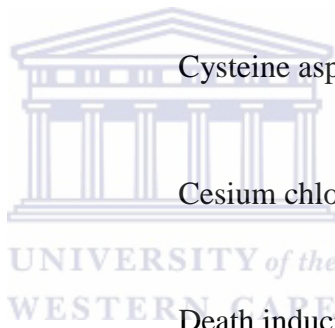
Figure 4.5: Binding of p6.1-Qdot 525 conjugate to cancer cells.....89

Figure 4.6: Binding of p.L-Qdot 525 conjugate to cancer cells.....90

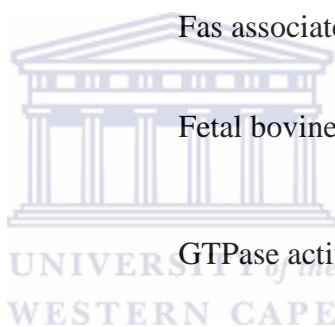


ABBREVIATIONS

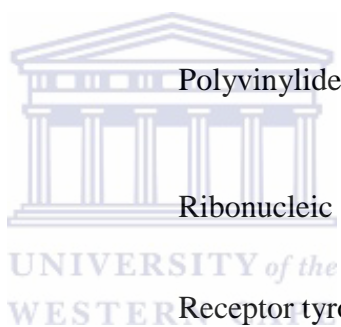
AIF	Apoptosis inducing factor
APC	Adenomatous polyposis coli
Aps	Ammonium persulphate
Apaf-I	Apoptosis protease activating factor
CDK	Cyclin dependent kinases
Caspases	Cysteine aspartic acid-specific proteases
CsCl	Cesium chloride
DISC	Death inducing signaling complex
DMEM	Dulbecco's modified eagle's medium
DMSO	Dimethyl sulfoxide
DNA	Deoxyribonucleic acid
DTT	Dithiothreitol



EDC	1-ethyl-3-(3-dimethylamino) carbodiimide HCl
EDTA	Ethylene diamine tetra-acetic acid
EGFR	Epidermal growth factor
EMT	Epithelial-mesenchymal transition
ExPASy	Expert protein analysis system
FADD	Fas associated death domain
FBS	Fetal bovine serum
GAP	GTPase activating protein
GDP	Guanosine diphosphates
GNP	Guanine nucleotide factor
GTP	Guanosine Triphosphates
GTE	Glucose-Tris-EDTA
KAc	Potassium acetate
kDa	Kilodalton



kb	Kilobase
MAPK	Mitogen activated protein kinase
NaCl	Sodium chloride
NaOH	Sodium hydroxide
PBS	Phosphate buffered saline
PDGF	Platelet derived growth factor
PVDF	Polyvinylidene difluoride
RNA	Ribonucleic acid
RTK	Receptor tyrosine kinase
SDS	Sodium dodecyl sulphate
SDS PAGE	Sodium dodecyl sulphate polyacrylamide gel electrophoresis
TBS-Tween	Tris-buffered saline containing Tween 20
TEMED	N,N,N',N'-Tetramethylethylenediamine
TGF- β	Transforming growth factor beta



TNF

Tumor necrosis factor

v/v

volume to volume

w/v

weight to volume



ACKNOWLEDGEMENTS

I would like to express my sincere gratitude to Dr Mervin Meyer for presenting me the opportunity to carry out this research. The guidance, patience and supervision he provided were invaluable and created an excellent atmosphere for me to carry out the research project. I would like to thank the University of Western Cape for providing excellent research facilities as well as the Nanotechnology Innovation Centre for funding.

I would like to acknowledge the following people for adding value to the thesis; Dr Zukile Mbita, Mr Francois Taute, Dr Paul Abidemi, Ms Morounke Saibu, Ms Nteveleni Thovhogi and Ms Rumbi Mudzonga. I would also like to thank the Biotechnology staff members and students who certainly made this a pleasant journey.

Special thanks goes to the special people in my life; my mother Monica for being a pillar of strength and a source of big encouragement, thanks to my father Langson, to my husband Aubrey for your patience love and understanding, to my siblings Miria, Melanie and Mushinka for all the love and encouragement and to my baby Mambo Mainza for all the joy you have brought in my life.



UNIVERSITY *of the*
WESTERN CAPE



UNIVERSITY *of the*
WESTERN CAPE

CHAPTER 1: INTRODUCTION

1.1. Background

Cancer has been identified as the leading cause of death in developed countries and the second leading cause of death in developing countries (WHO, 2008). According to the global cancer statistics conducted by GLOBOCAN, there were 12.7 million new cases of cancer and there were 7.6 million deaths as a result of cancer in 2008 (Jemal *et al.*, 2011). Of these, 7.1 million new cases and 4.9 million deaths from cancer occurred in developing countries. In Africa there were 667,000 new cases of cancer and 518,000 deaths comprising 5% of the global cancer incidence and 7% of the global cancer mortality rate (WHO, 2008). The low rates give the impression that the cancer burden is very low in Africa; however it is possible that this is not a true reflection of the cancer burden. This is because data collection in most African countries only covers subsections of the total population usually urban areas. Hence the data from which incidence and mortality rates are calculated are considered of poor quality (Ferlay *et al.*, 2010). It is very much a possibility that the cancer burden in Africa and other developing countries is much higher. In South Africa, the estimated number of cases of cancer was 58,000 and the deaths from these cancers was 40,000 every year as of 2002 (Mayosi *et al.*, 2009). Lung cancer was identified as the leading cause of death in men with 13% of all cancer deaths. This was followed by Kaposi's sarcoma and esophageal cancer causing 11% of cancer deaths. Cervical cancer was identified as the leading cause of death in women with 20% of cancer deaths. This was followed by breast cancer with 15% and Kaposi's sarcoma causing 6% of cancer deaths (Mayosi *et al.*, 2009). While statistics show that mortality rates in developed countries are on the decrease, the inverse is true in developing countries. This can be attributed to poor medical facilities, treatment options and late diagnosis of

cancer (WHO, 2008). If detected early cancer can be treated successfully. Hence to reduce mortality rates especially in developing countries, developing better diagnostic systems for cancer detection is vital. The development of these diagnostic systems depends on the unravelling of the cellular and molecular etiology of cancer.

1.2. Molecular biology of cancer

Cancer has been defined as several distinct diseases that manifest as malignant tumors (Fujimura, 1988). These diseases are due to genetic changes or mutations and epigenetic changes. These result in various phenotypic characteristics that result in malignant neoplasia.

1.2.1. Genetic changes

Development of tumors or tumorigenesis is a multistep process. This process is exemplified by a linear model proposed by Fearon and Vogelstein. In this model hyperproliferation of cells is preceded by normal cells leading to dysplastic cells as shown in Figure 1.1. This is followed by formation of an adenoma and eventually carcinogenesis and metastasis (Fearon and Vogelstein, 1990).

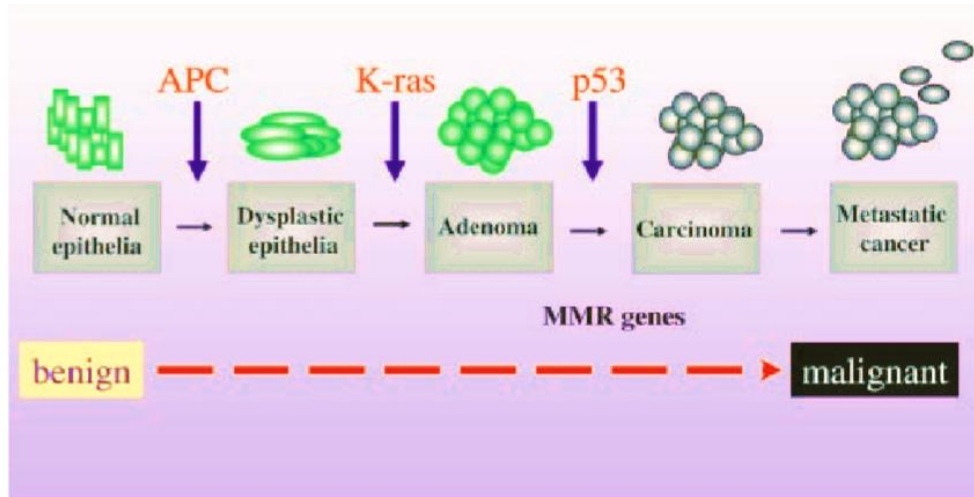


Figure 1.1: Tumorigenesis development model. The APC, K-ras gene and p53 genes are mutated along different neoplastic transformations in the development of metastatic cancer in colorectal cancer (Adapted from Smith *et al.*, 2002).

Pivotal in this multistep process of cancer development are the genetic mutations that occur at each step into the next stage of development. The genes mutated include the adenomatous polyposis coli (APC) gene, the Kirsten-ras (K-ras) gene and the p53 gene as shown in (Fearon and Vogelstein, 1990). It has been suggested that accumulations of mutations rather than the order of the mutations is important for an adenoma to progress to a carcinoma (Smith *et al.*, 2002). The APC gene is located on chromosome 5q21 and encodes a 312kDa (APC) protein. The APC protein possibly functions in protein-protein interactions that regulate phosphorylation and degradation of β -catenin and is modulated by the WNT signaling pathway (Näthke, 2004). Phosphorylation of β -catenin by the APC protein controls the amount of β -catenin that is available for activation of transcription factors. Other proteins that are part of the pathway include GSK3 β , axin and several kinases (Näthke, 2004). In the absence of WNT extracellular signals, GSK3 β as part of the APC- β -catenin-axin complex becomes active. This leads to phosphorylation of the aforementioned

proteins and interactions between the proteins is increased. This in turn leads to binding of ubiquitin and eventual destruction of the cell by proteasomes (Näthke, 2004). In the presence of WNT signal GSK3 β is inactivated resulting in an increased amount of β -catenin which leads to activation of transcription factors. Accumulation of β -catenin also occurs when truncation mutations occur in the APC gene. These mutations make it impossible for β -catenin to bind to the APC protein and hence β -catenin accumulates leading to activation of genes that play a role in cell proliferation and differentiation (Smith *et al.*, 2002).

The K-ras oncogene has been reported in approximately 30% of colorectal cancers (Liu *et al.*, 2011). The K-ras gene encodes a 21kDa (K-ras) protein that is activated in response to stimuli such as cytokines and hormones. The K-ras protein functions by catalyzing the hydrolysis of guanosine triphosphates (GTP) to guanosine diphosphates (GDP) and results in the turning off of the associated pathways (Shaw *et al.*, 2011). K-ras mutations commonly occur in codon 12 and 13 (Chang *et al.*, 2010). The activation mutations commonly seen are G to A transitions and G to T transversions. K-ras genes are known to be associated with cytokine signaling, cell adhesion, survival, proliferation and apoptosis. Failure in the regulatory role of K-ras gene as determined by mutations contributes to the development of carcinomas (Liu *et al.*, 2011).

The gene *p53* is thought to be mutated in 70% of colorectal carcinomas and mutations of *p53* gene are thought to be a late event in the development of cancer. Found on chromosome 17, *p53* functions by transcribing for transcription factors that regulate the cell cycle by binding to a variety of genes such as p21 Bax and Bcl-2 as a response to DNA damage and other stresses (Smith *et al.*, 2002). The tumor model suggested by Fearon and Vogelstein paved way for discovery of cancer related genes namely oncogenes and tumor suppressor genes (Fearon and Vogelstein, 1990).

1.2.1.1. Oncogenes

Mutations in normal functioning genes called proto-oncogenes give rise to oncogenes. In normal cells, proto-oncogenes perform various functions which include coding for proteins that stimulate cell division as well as inhibition of cell differentiation and proliferation (Novakofski, 1991).

Oncogenes encode products that promote tumorigenesis by conferring cell growth advantages leading to increased cell proliferation and survival. Oncogenes become activated in three main ways namely chromosomal rearrangements, mutations and gene amplifications (Anderson *et al.*, 1992). Chromosomal rearrangements usually involve translocations. Translocations result in the relocation of a proto-oncogene to a new chromosomal site leading to higher expression of genes. Fusions between proto-oncogenes and a second gene also occur due to translocations and this results in a fusion protein with oncogenic activity (Chial, 2008). Mutations that occur in proto-oncogenes are in the form of point mutations, deletions or insertions. These mutations lead to hyperactive gene products and mutations in the promoter region of proto-oncogenes leads to increased transcription. Gene amplification leads to production of multiple chromosomal copies of proto-oncogenes (Chial, 2008). An example of an oncogene is the Ras oncogene. The members of the Ras genes include H-ras, K-ras and N-ras and these genes encode GTPases (Bodemann and White, 2013). The Ras proteins function by acting as molecular switches that regulate the state of GTP and GDP phosphorylation. In the basal state, Ras protein is GDP bound. The Ras protein becomes phosphorylated when activated by receptor tyrosine kinases (RTKs) recruit guanine nucleotide factors (GEFs). When phosphorylated the Ras protein signals downstream pathways which include mitogen activated protein kinase (MAPK) and phosphoinositide 3 kinase pathways (Young *et al.*, 2013). These pathways are important for the regulation of cell growth. The Ras protein returns to its basal state by hydrolysis of GTP through the GTPase activating protein

(GAP). Mutations in the Ras genes play a role in cancer development (Young *et al.*, 2013). Mutations are in the form of point mutations that occur at positions 12, 13 or 61 on the Ras allele (Chang *et al.*, 2010). Mutations of these genes results in production of active proteins that continually sends transducing signals resulting in uninhibited cell growth (Goodsell, 1999). An example is the amplification of recombinant human tyrosine kinase receptor isoform 2 (ErbB2) as seen in breast cancer and is associated with poor prognosis (Carlo and Croce, 2008). Products of oncogenes include growth factors, growth factor receptors, transcription factors and serine threonine kinases.

1.2.1.1.1. Growth factor and Growth factor receptors

Growth factors stimulate growth by binding to growth factor receptors on cells. In normal conditions these factors are produced by one cell type and act on receptors of another cell type. In neoplasia, growth factors are self-produced by cancer cells in an autocrine fashion. These factors then stimulate growth factor receptors on the cells from which they are produced (Heldin and Westermark, 1999). An example of an oncogenic growth factor is the platelet derived growth factor (PDGF). PDGF is released by platelets during coagulation and functions by inducing proliferation of fibroblasts which promote wound healing. Overexpression of PDGF gives rise to tumors which include gliomas and fibrosarcomas (Andrae *et al.*, 2008). Growth factor receptors also known as RTKs consist of an extracellular ligand binding domain, a transmembrane domain and the intracellular cytoplasmic domain. An example is the epidermal growth factor receptor (EGFR). Mutations in the extracellular domain results in activation of this receptor. The implication is that the receptor no longer requires ligand binding for downstream signaling and as such the intracellular domain continually phosphorylates tyrosines providing interaction sites for proteins with the Src homology 2 domain (SH2) (Arteaga, 2002). Several signaling pathways are activated

by these interactions. These lead to activation of oncogenes such as Ras oncogenes. Mutations of the ErbB2 growth factor receptor are associated with poor prognosis as seen in breast cancer (Bargmann *et al.*, 1986).

1.2.1.1.2. Serine/threonine kinases

Activated Ras oncogenes promote transcription of genes that in turn promote cell growth and proliferation by binding to GTP (Vojtek and Der, 1998). Activation of the Ras oncogenes further leads to signaling of molecules known as serine threonine kinases for example the Raf oncogenes. Once activated, the Raf oncogenes activate genes that encode the mitogen induced protein kinases (MAPKs). These kinases promote vessel permeability and eventually cell proliferation (Goodsell, 1999).



1.2.1.1.3. Transcription factors

The best known example of an oncogene that encodes a transcription factor associated with tumorigenesis is myelocytomatosis viral oncogene (MYC). MYC encodes the transcription factor c-Myc which is a DNA binding transcription factor (Koskinen and Alitalo, 1993). C-Myc is a basic loop helix that forms a heterodimer with max protein (Blackwood and Eisenman, 1991) and binds to sequences near the promoter region. In normal cells, c-Myc promotes cell growth and proliferation by controlling growth factor stimulation. However in cancer cells over expressing c-Myc, growth factor stimulation is by passed thereby promoting tumor development (Lin *et al.*, 2012).

C-Myc promotes tumorigenesis by actively binding to the core promoters of actively transcribed genes. It also binds to enhancers that are associated with the core promoters of active genes as well as transfer RNA (tRNA) and ribosomal RNA (rRNA). C-Myc also binds moderately to genes that are not being transcribed (Lin *et al.*, 2012)

In cells that overexpress c-Myc, total RNA levels are increased in contrast to RNA levels in normal cells. This indicates that the primary role of c-Myc in cancer development is amplified transcription of already actively transcribed genes. C-Myc gene transcription has been seen in various cancers such as multiple myeloma, glioblastoma multiform and small cell lung carcinoma (Lin *et al.*, 2012).

1.2.1.2. Tumor suppressor genes

Tumor suppressor genes are genes that encode proteins that control cell division, by repairing damaged DNA. Others control the adhesion of cells to each other as well as to the extra cellular matrix. Tumor suppressor genes also encode proteins that act in signaling pathways that control the cell cycle. Mutations in tumor suppressor genes lead to the development of cancer (Zhao *et al.*, 2012). The best known example of a tumor suppressor gene is *p53* which encodes the p53 protein. The role of p53 includes activation of DNA repair, cell cycle arrest at the G1 and S phases as well as initiation of apoptosis (Bai and Zhu, 2006). In response to cellular stress, p53 functions by up regulating the transcription of the WAF/CIP1 gene. This gene encodes the protein p21, which binds to Cyclin Dependent Kinases (CDK) complexes. Binding of p21 to CDK complexes results in cell cycle arrest at the G1 and S phases (Chen *et al.*, 1996). Cell cycle arrest allows for DNA repair to occur and failure of successful DNA repair drives the cell into apoptosis. Mutation in the *p53* gene can result in an unfunctional p53 protein that cannot bind DNA. As a result p21 is not

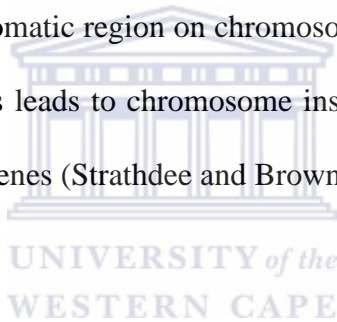
transcribed and uncontrolled cell proliferation results in tumor formation. Mutations of p53 have been reported in more than half of human cancers (Ikeguchi *et al.*, 2000).

1.2.2. Epigenetic changes

Epigenetics has been described as stable modifications in gene expression without any alterations in the gene sequence (Martinez *et al.*, 2003). The most common epigenetic event that has been widely studied is DNA methylation. DNA methylation involves the addition of a methyl group to the cytosine ring at position 5. In mammals DNA methylation plays a role in development particularly embryogenesis and gametogenesis (He *et al.*, 2011). DNA methylation occurs at CpG residues and is catalyzed by DNA methyltransferases (Deaton and Bird, 2011). The human genome is largely deficient of CpG residues and where these residues are present they are methylated. There are however regions in the genome that are rich in CpG residues and these are called CpG islands. The CpG islands are mainly found near promoter regions and are largely unmethylated (Deaton and Bird, 2011). Approximately 70% of gene promoters are associated with CpG islands and these genes include housekeeping gene, tissue specific genes and developmental regulator genes and some serve as tumor suppressor genes. The unmethylated state of these genes allows for transcription to occur (Baylin *et al.*, 2001).

Tumorigenesis occurs when the CpG islands become hypermethylated and this leads to silencing of tumor suppressor genes (Bird and Wolffe, 1999). Loss of gene function is exemplified by GSTP1 gene which encodes glutathione-S-transferase and plays a role in detoxifying electrophiles that damage DNA. Loss of expression of GSTP1 leads to increased oxidative stress which damages DNA and promotes tumorigenesis. Loss GSTP1 gene expression has been seen in most tumors and further examination of these tumors has revealed hypermethylation in the promoter regions (Grimminger *et al.*, 2012).

Another contributory factor as a result of epigenetics is hypomethylation. Hypomethylation is the loss of methylation at normally methylated regions in a genome (Lin *et al.*, 2011). Areas that are normally methylated include satellite areas and retrotransposons. Satellite areas are tandem repeats of non-coding DNA that form the main component of heterochromatin (Kim *et al.*, 2009). Retrotransposons are a subclass of transposons and they function to increase the copy number of transposons there by increasing the genome size. Retrotransposons also encode reverse transcriptase which is an enzyme involved in DNA replication via RNA (Cordaux and Batzer, 2009). Demethylation occurs when the enzyme deaminase converts the cytosine at position 5 to thymine followed by a thymine – guanine mismatch that replaces thymine. Hypomethylation occurs in the pericentric heterochromatic region on chromosome 1 and 9 as seen in breast cancer (Strathdee and Brown, 2005). This leads to chromosome instability and oncogene activation as seen in the H-ras and c-Myc oncogenes (Strathdee and Brown, 2005).



1.3. Distinguishing characteristics of cancer

Cancer is distinguished by four characteristics. These are also known as the hallmarks of cancer. They include cell cycle deregulation, apoptosis evasion, immortalization of cancer cells as well as tissue invasion and metastases. These characteristics are based on altered gene expression which results in altered protein profile. These proteins can be used as biomarkers to diagnose cancer.

1.3.1. Cell cycle deregulation

Cell division is a highly ordered process in which cell size, DNA integrity as well as extra cellular growth signals are evaluated through multiple check points in the cycle of a cell (Schmidt, 2007). The cell cycle comprises of four phases namely the mitotic (M) phase, the G1 phase, the G2 phase and the S phase as illustrated in Figure 1.2. DNA synthesis occurs at the G1 phase while replication takes place during the S phase (Martinez *et al.*, 2003). The cell prepares for mitosis in the G2 phase and in the M phase, the daughter progeny of the cell are produced by the segregation of the chromosomes. These processes culminate in cell division which occurs following cytokinesis (Singhal *et al.*, 2005; Schmidt, 2007). The cell cycle is regulated at various check points primarily by proteins known as CDKs (Keaton, 2007).

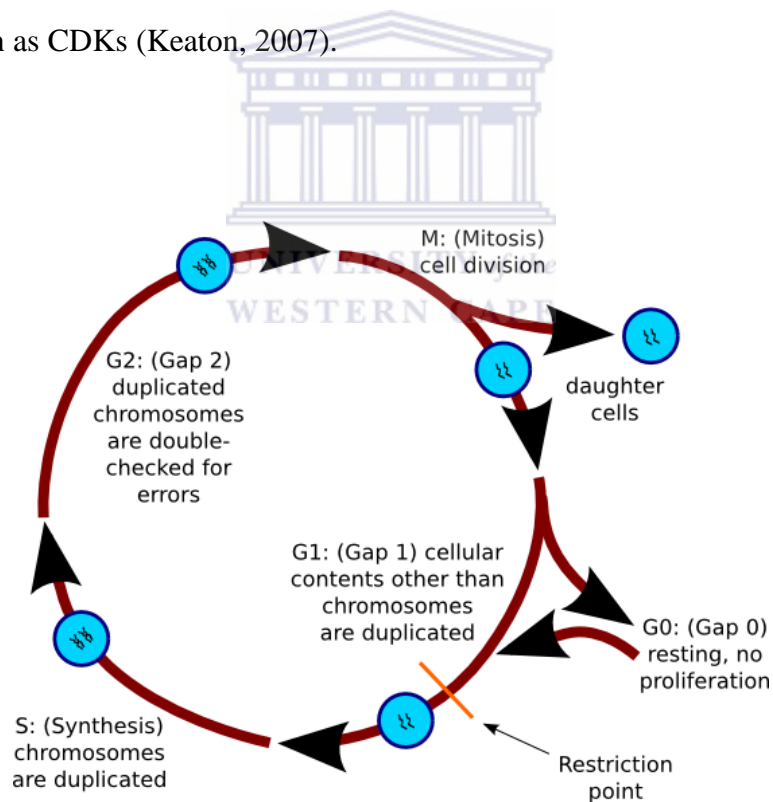


Figure 1.2: The cell cycle. Cell cycle consists of the M, G1, G2 and the S phase. Mitosis and DNA replication take place at the M and S phase (<http://www.newearthbiomed.org.145/chemo-article>).

Anti-cancer signals are signals that regulate the cell cycle. These signals include soluble growth inhibitors and immobilized growth inhibitors found in extra cellular matrix and they function to prevent cell proliferation. An example of this is transforming growth factor beta (TGF- β) (Harrington, 2007).

A protein that is central in the prevention of proliferation is the retinoblastoma protein (pRb). The pRb protein controls the progression in the cycle of a cell from the G1 phase into the S phase. In its unphosphorylated form, the pRb protein prevents proliferation of cells by binding the transcription factor, E2F/DP-1 (Hanahan and Weinberg, 2000; Shingal *et al.*, 2005). Phosphorylation of the pRb protein can occur via the activation of CDKs. This results in the release of E2F and transcription of genes that regulate DNA metabolism takes place. E2F is also released when the pRb protein is mutated or when it is not expressed and the end result is cell proliferation.

TGF- β prevents the phosphorylation of the pRb protein by blocking the action of cyclin and CDKs. Cancerous cells become insensitive to TGFs by loss of TGF- β receptors or by production of dysfunctional receptors through mutations. Some cancer cells over express cyclins and CDKs. The result is that the cell cycle is disrupted, hence giving rise to tumors (Harrington, 2007).

1.3.2. Apoptosis evasion

Apoptosis or programmed cell death is the process by which cells are destructed via a process in which cysteine aspartic acid-specific proteases (caspases) are activated. Apoptosis is characterized by cell shrinkage, membrane blebbing, nuclear condensation and fragmentation (Zornig *et al.*, 2001).

Cells are eliminated via apoptosis when they are no longer needed or when their DNA is damaged extensively (Askenazi and Dixit, 1999). Apoptosis is effected via two pathways namely the intrinsic or mitochondrial pathway and the extrinsic or death receptor initiated apoptosis pathway.

1.3.2.1. The intrinsic or mitochondrial pathway

Mitochondria are involved in apoptosis through the regulation of cytochrome *c* (Ozoren and El-Derry, 2003). In this pathway the outer membrane of the mitochondria is perturbed by activation of caspases through the proapoptotic members of the Bcl family. When the outer membrane becomes disrupted, protein from the intermembrane space which include cytochrome *c*, smac/DIABLO, AIF and endonucleases are released into the cytoplasm. This leads to activation of caspase 3 which is activated by cytochrome *c* (Zornig *et al.*, 2001).

Cytochrome *c* binds to Apaf-1 through association with dATP and this is followed by recruitment of initiator caspases to form the *c*/Apaf-1/caspase 9 apoptosome complex. Once this complex is formed, caspase 3 is recruited to the complex and becomes activated by caspase 9. Activated caspase 3 then cleaves substrates in the cells and eventually apoptosis takes place as shown in Figure 1.3 (Ozoren and El-Derry, 2003).

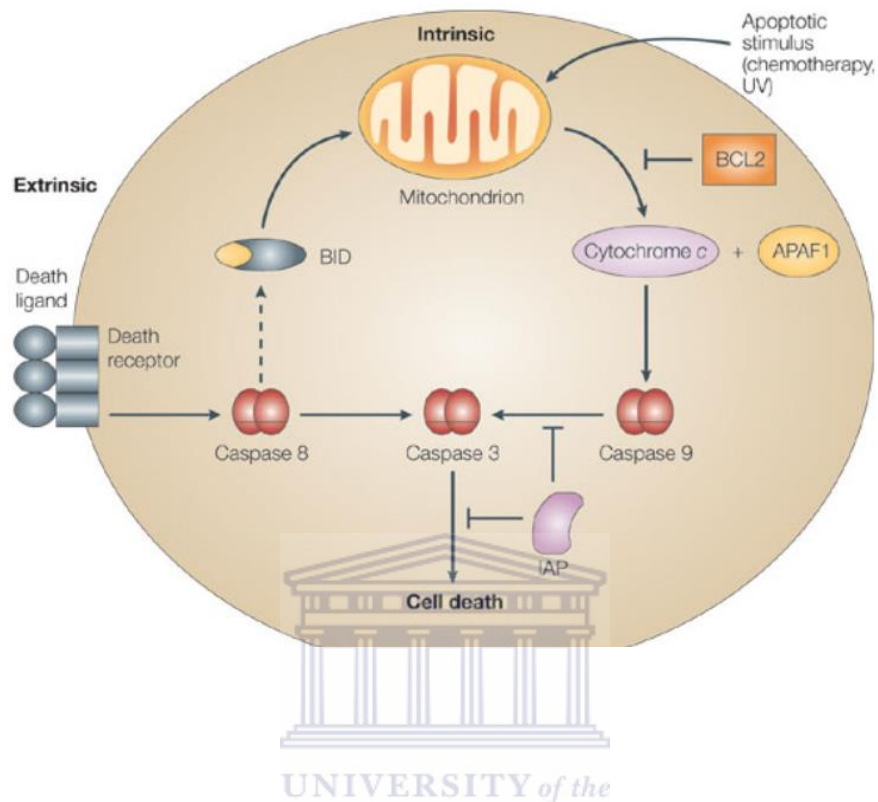


Figure 1.3: The extrinsic and intrinsic pathway involved in apoptosis. Caspase 8 is activated via ligand binding to the death receptor while cytochrome c is released from the mitochondrion following stress. These events eventually lead to activation of caspase 3 and apoptosis occurs (Adapted from Anderson *et al.*, 2005).

1.3.2.2. Extrinsic pathway or the death receptor pathway

Protein receptors of the family tumor necrosis factor (TNF) also known as death receptors, are involved in the extrinsic pathway of apoptosis. Examples of the receptors are TNF receptor (TNF-R1), CD95 (APO-1/Fas), TNF related apoptosis-inducing ligand receptor (TRAIL-1/2) and DR6 (Askenazi and Dixit, 1999). Their corresponding ligands include CD95 ligand (CD95L) and TNF α . Stimulation of these receptors by a ligand, trigger a variety of cellular responses among them proliferation, differentiation and apoptosis (Zornig *et al.*, 2001). The extrinsic pathway is

here exemplified by the CD95 receptor. CD95 is activated through its death domain (DD) by ligand binding. Upon stimulation the receptor recruits Fas associated death domain (FADD) and FADD recruits caspase 8 to the CD95 receptor. This results in the formation of a complex known as CD95 death-inducing signaling complex (DISC). Caspase 8 causes activation of downstream effector caspase 3 and this eventually leads to apoptosis as shown in Figure 1.3 (Ozoren and El-Derry, 2003; Fulda and Debatin, 2004; Budd, 2002).

Cancer arises when cells evade apoptosis. Apoptosis evasion results when there is disruption of death receptor pathways in the extrinsic pathway. This occurs due to down regulation of expression of death receptors as is seen in down regulation of CD95 in neuroblastoma (Friesen *et al.*, 1997). Mutations in CD95 have also been identified in various tumors and these mutations prevent binding of CD95L to the CD95 receptor. Also other receptors known as decoy receptors such as DcR3 are over expressed in cancers. The result is that CD95L binds with higher affinity to DcR3 rather than CD95 and hence apoptosis is inhibited (Roth *et al.*, 2001).

Disruptions due to mutations also occur in the intrinsic pathway. Apoptosis is evaded when Bcl-2 is overexpressed due to chromosomal translocation of the bcl-2 oncogene in the immunoglobulin heavy chain gene locus. This type of translocation has been seen in human follicular lymphoma (Young *et al.*, 2008). Mutations in the *p53* gene also affect the intrinsic pathway. This occurs through the upregulation of p53 responsive elements such as BH3. P53 also binds to Bcl-X and Bcl-2 at the mitochondria thereby promoting destabilization of the mitochondrion membrane (Mihara *et al.*, 2003).

1.3.3. Cell immortality

In comparison to normal somatic cells, cancer cells have the ability to replicate indefinitely. Somatic cells are unable to replicate indefinitely due to telomere attrition or shortening of the telomeres (Junknecht, 2004). Telomeres are specialized structures made of nucleic acids, found at the ends of chromosomes where they serve as capping structures. Telomeres protect chromosomes from degradation as well as end to end fusion. Telomeres comprise of a repetitive sequence of DNA namely TTAGGG in humans (Kelland, 2005). During replication about 50-200 base pairs of telomeres are lost during each replication cycle. Eventually telomeres shorten to a critical point such that the replicative potential of the cell is limited and growth arrest occurs (Junknecht, 2004). Tumor cells however have the ability to maintain telomere length and hence replicate indefinitely or become immortal. Tumor cells are able to repair their telomeres by the activation of a reverse transcriptase mechanism using the enzyme telomerase. The enzyme adds a TTAGGG unit to the ends of the telomeres and the result is that telomere length is maintained and replication of the cells takes place indefinitely (Bearss *et al.*, 2000).

1.3.4. Metastasis

Progression of a tumor is measured by the ability of the tumor to leave its confined space and spread. Primary progression occurs when a tumor invades surrounding healthy tissue through the basement membrane. Subsequent progression occurs when tumor cells enter the blood stream, migrate and settle in other parts of the body to form secondary tumors. This process is called metastasis (Zhang *et al.*, 2008).

Metastasis is thought to occur through a process called epithelial-mesenchymal transition (EMT). EMT proceeds when tumor cells invade and breaks down the basement membrane. This occurs through the formation of invadopodia on the tumor cells. Invadopodia are protrusions that degrade the basement membrane through actin polymerization (Bravo-Codero *et al.*, 2012).

Actin polymerisation occurs through signaling pathways that are linked to the Rho family of GTPases (Neel *et al.*, 2012). In particular the small GTPases RalA and RalB have been shown to be involved in metastasis through invadopodia formation. This was demonstrated by depleting pancreatic ductal adenocarcinoma cells (PDAC) of endogenous RalA and RalB by using shRNA (small hairpin RNA). The cells showed significant decreases in numbers of invadopodia on the cells as well as a decrease in invadopodium positive cells (Neel *et al.*, 2012).

Once cancer cells compromise the basement membrane through invadopodia, they enter circulation and develop the ability to evade the immune system until they reach their destination. Once they reach their destination, the cancer cells exit the capillaries by degradation. They then settle in their new environment and begin to proliferate (Hanahan and Weinberg, 2000).

1.4. Cancer diagnosis

Effective cancer detection depends on development of diagnostic methods that can detect cancer at its inception stages. Currently cancer is detected using various methods. These include faecal occult blood test for colorectal cancer (Rabaneck *et al.*, 2008), surgical biopsy, mammography as well as computed axial tomographic (CAT) scan. These methods however are associated with several limitations. For example while mammographs are designed to detect cancer at early stages, 30% of breast cancers still go undetected. Also mammographs are known to produce false positive results (Manning, 2004; Noel *et al.*, 2007). While CAT scans produce images of high resolution that allow for early cancer detection, they employ the use of contrasting agents which have adverse effects such as nausea, kidney failure as well as severe allergic reactions (Brenner and Hall, 2007). Surgical biopsy is used to detect cancer using histology and cytology techniques. Apart from the inability of this method to detect cancer at early stages, surgical biopsy is invasive and causes physical and psychological distress to the patient (Sarbeni *et al.*, 2007; Iglesias-Garcia *et al.*, 2007). Current diagnostic methods are also costly and not readily available to an average individual (Choi, *et al.*, 2010). Therefore it is of utmost importance that a diagnostic method that can detect cancer at early stages, a method that is affordable and readily available is developed. Understanding of molecular and cellular etiology of cancer has opened up avenues that are being employed in the development of powerful diagnostic methods. These include amongst others the use of cancer biomarkers and nanotechnology.

1.5. Cancer biomarkers

A biomarker has been defined as a distinctive feature that can be measured objectively to give an indication of normal biological processes, pathological processes as well as pharmacologic responses to a therapeutic intervention (Mishra and Verma, 2010). There are several categories of biomarkers. The most common category of biomarkers are molecular biomarkers which constitute genetic biomarkers, epigenetic biomarkers as well as molecular targets (Research advocacy network, 2010). Mutations in genes that regulate cell proliferation and several homeostatic functions serve as genetic markers. Examples of these genetic markers include *p53*, Rb, BRCA-1 and BRCA-2 (Godefroy *et al.*, 2006).

Epigenetic changes which constitute modification of genes resulting in altered gene expression have also been implicated in cancer initiation (Bhatt *et al.*, 2010). DNA hypomethylation and hypermethylation has been associated with stronger gene expression and gene silencing respectively, both of which are tumor promoting events. Examples of genes affected by methylation include Rb and APC genes (Baylin *et al.*, 2001).

Molecular pathways that promote cell proliferation and prevent apoptosis have also been identified as cancer biomarkers. As such these pathways are being utilized for targeted cancer therapy as well as diagnosis. These biomarkers include receptor kinases such as EGFRs (Citri *et al.*, 2002). Recently these receptors are being utilized for cancer diagnosis using nanotechnology (Mousa and Bharali, 2011).

1.6. Cancer targeting peptides

A study carried out by St Croix and others aimed to study genes that were expressed in human tumor endothelium (St Croix *et al.*, 2000). Of the 170 transcripts studied 79 were differentially expressed in comparison to transcripts in normal cells. It was also found that 46 of these transcripts were specifically elevated in tumor endothelium. This study and others showed that genes in tumor cells and normal cells are differentially expressed resulting in different cell surface proteins. These proteins include cell receptors, adhesive molecules as well as growth factors (Shadidi and Sioud, 2003).

Cell surface proteins have been the focus of cancer targeting initially using monoclonal antibodies. Examples of these cell surface proteins include mucins. Mucins are high molecular weight glycoproteins that are found in the epithelial tissue. They have a high content of clustered oligosaccharides and are linked to tandem repeat peptides that are rich in threonine, serine and proline. Mucins are over expressed in colorectal cancers (Byrd and Bresalier, 2004). Antibodies have been useful as tumor targeting agents for cancer diagnosis. Kruglyak and others used the antibody Tag-72 monoclonal antibody (CYT-103) that has high binding specificity to mucins to detect colorectal cancer (Kruglyak *et al.*, 1997). The antibody was conjugated to radioactive indium III and administered to a patient suspected of having colorectal cancer. A CT scan was obtained and revealed a single focus of increased uptake along the inferomedial edge of the liver. A subsequent endoscopy revealed a 3 cm tumor. A prior CT scan without administration of Indium-III CYT-103 did not show any abnormal activity (Kruglyak *et al.*, 1997). Antibodies however have limitations for use as targeting agents in this regard. Antibodies are quite large molecules that have difficulty in penetrating cancer cells and tumors. Monoclonal antibodies also

have regions that bind to the reticuloendothelial system and as such, use of them to deliver cytotoxic agents could lead to systemic toxicity (Aina *et al.*, 2002).

An alternative to the use of monoclonal antibodies in cancer targeting or diagnosis is the use of peptides. Peptides are attractive as cancer diagnostic molecules as they bind selectively to specific molecules on cancer cells. Due to their small size cancer targeting peptides are able to evade the immune system unlike antibodies (Shadidi and Sioud, 2003). Methods employed in the identification of cancer targeting peptides include molecular modelling and bio-panning. Unlike bio-panning, molecular modelling relies on prior knowledge of the receptor or related receptor structure. Bio-panning involves incubation of a phage library with the desired targets. Phages that do not bind strongly to the receptor on cells are washed away while bound phages are collected by elution and then propagated in *Escherichia coli*. These phages are subjected to further rounds of selection to obtain a peptide with high binding specificity (Shadidi and Sioud, 2003).

Several cancer targeting peptides and some of their corresponding receptors have been identified. These include KCCYSL (Karasseva *et al.*, 2002), MYWGDSHWLQYWYE (Urbanelli *et al.*, 2001) and LTVSPWY (Shadidi and Sioud, 2003). The KCCYSL peptide (designated p6.1) was discovered by Karasseva and others from a phage display library (Karasseva *et al.*, 2002). This library was raised against recombinant human ErbB2-EDC which is an extracellular domain of the ErbB2 receptor. These results demonstrated that p6.1 peptide bound with high specificity to ErbB2 receptors in prostate cancer cells. As such this peptide is an attractive vehicle to deliver cytotoxic drugs and can also be used in diagnostics.

The MYWGDSHWLQYWYE (designated NL1.1) was one of the first peptides that was shown to have a high binding specificity to HER2 or ErbB2 receptor. This peptide was discovered by Urbanelli and others using a phage display library (Urbanelli *et al.*, 2001). In this study the NL1.1 peptide bound with high specificity to a matrix with immobilized with HER2 protein. It was also shown that this peptide bound with high specificity to SkBr3 breast cancer cells and NIH3T3/neu fibroblasts transfected with human HER2 expression plasmid in comparison to human melanoma Mewo fibroblasts and NIH3T3 mouse fibroblasts. The SkBr3 breast cancer cells and the transfected NIH3T3 cell lines had high expression of ErbB2 receptor.

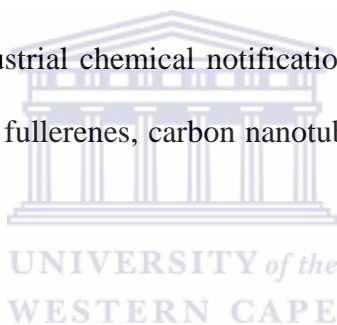
The phage derived peptide LTVSPWY was discovered among phage display library using a bio-panning protocol (Shadidi and Sioud, 2002). It was shown that the peptide of sequence LTVSPWY binds with high specificity to SKBR3 cells as well as T47D cancer cells, which are of breast origin. These cells showed a particularly high expression of the ErbB2 receptor. The authors further demonstrated that the peptide could be used as a delivery molecule. An antisense oligonucleotide was conjugated to LTVSPWY and peptide conjugate was internalized. This resulted in reduction of ErbB2 expression.

1.7. Introduction to Nanotechnology

The concept of nanotechnology was introduced by Richard Feynman who suggested that atoms could be arranged one by one to achieve new properties of a material (Feynman, 1960). In his letter ‘there is plenty of room at the bottom’ Feynman wrote that the properties of a material at atomic level behave differently to materials on a large scale. This is because at a small scale different laws of quantum mechanics apply (Feynman, 1960). Therefore nanotechnology operates at the primary

level of atoms and molecules. The purpose of nanotechnology is to construct nanoparticle materials from bottom up. The resulting materials are high performance materials due to the fact that the properties of the manipulated molecules change in comparison to the natural state (Bhattacharyya *et al.*, 2009; Guz and Rushchitsii, 2003).

According to the International Union of Pure and Applied Chemistry (IUPAC), a nanoparticle is a particle of any shape with dimensions in the 1×10^{-9} m and 1×10^{-7} m range (Vert *et al.*, 2012). Therefore there is a 100 nm limit on a nanoparticle because the unique properties of these materials develop at critical length scale of 100 nm (Vert *et al.*, 2012). The unique properties of nanoparticles include increased surface area, increased chemical reactivity, novel optical properties and magnetic properties (National industrial chemical notifications and Assessment scheme, 2006). Examples of nanoparticles include fullerenes, carbon nanotubes and quantum dots (Wang *et al.*, 2008).



1.7.1 Quantum dots

Quantum dots are crystals that are nanometre sized and are composed of a core, a shell and an outer coating as shown in Figure 1.4. The cores of quantum dots are made from elements of groups II-VI (Cadmium Selenide, CdSe) or groups III-V (Indium phosphorous, InP). The core of quantum dots is covered by a semiconductor material, the most commonly used being Zinc Sulphide (ZnS). It stabilizes the core and improves the optical properties of the quantum dot by increasing the spectral band gap (Azzazy *et al.*, 2007). Quantum dots are made functional by coating the shell with a polymer such as octylamine-modified polyacrylic acid. This polymer interacts with Trioctylphosphine oxide (TOPO) on the surface of the shell through alkyl groups. Quantum dots are thus rendered amphiphilic due to the carboxylic groups that face away from the core of the quantum dots (Smith *et al.*, 2004).

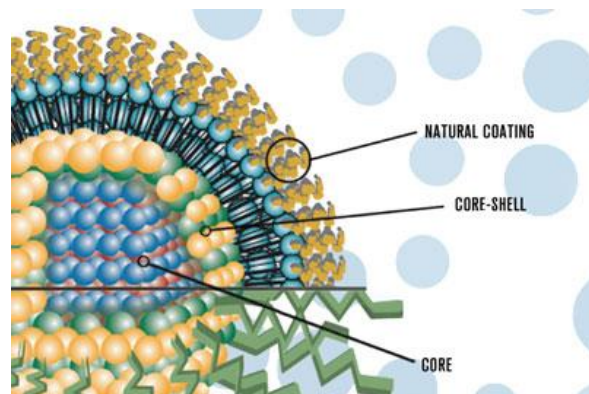


Figure 1.4: Structure of a quantum dot. The core of the quantum dot is made of material from group II and VI such as CdSe while the shell is made from semi conducting material such as ZnS (www.the-scientist.com/article/display/15458)

Quantum dots were initially described in 1982 when they were prepared for use as probes for investigation of surface kinetics. In these studies it was found that quantum yields of the quantum dots was affected by molecules attached to their surface (Azzazy *et al.*, 2007; Smith *et al.*, 2004). Studies carried out in 1998, conducted by Alivisatos at UC Berkeley and another by Nie at Indiana University as reported by Smith and others showed that biomolecules could be conjugated to quantum dots and that these conjugated biomolecules could be made water soluble (Smith *et al.*, 2004). These findings paved way for biological studies involving molecular and cellular imaging.

1.7.1.1. Properties of quantum dots

Quantum dots have several properties which make them superior fluorophores in comparison to organic fluorophores. Quantum dots emit a range of fluorescence dependent on their size. As the size of the quantum dot increases the band gap or energy gap also increases. Consequently quantum dots emit light of wavelengths ranging from ultraviolet to infrared depending on size. As an example a quantum dot with size of approximately 2nm made of CdSe emits fluorescence in the range of 400-500nm while a 5nm quantum dot will emit fluorescence in the range 600nm (Figure 1.5) (Alivisatos *et al.*, 2005).

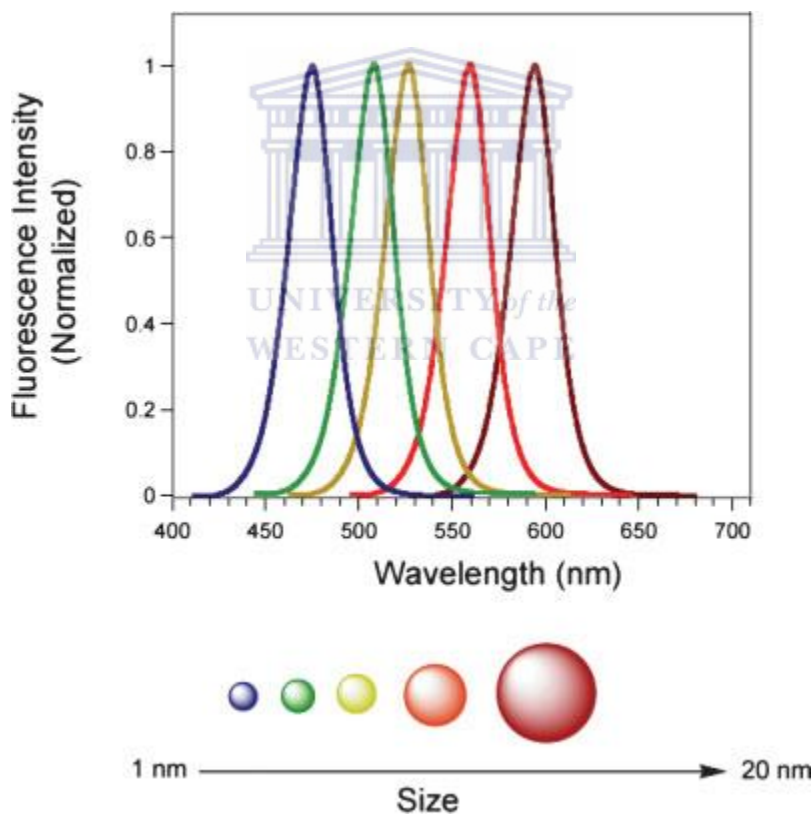


Figure 1.5: Quantum dot size and wave length relationships. Quantum dots fluoresce in wavelengths ranging from ultra violet to infra-red dependent on their size (Adapted from Zhou and Gosh, 2006).

Compared to organic fluorophores, quantum dots have broad absorption spectra and narrow emission spectra (Zhou and Ghosh, 2006). Quantum dots can be excited by almost any source of light, for example white light, ultraviolet light as well as blue-violet filtered light at a wave length of 405nm and 488nm (Azzazy *et al.*, 2007). As such several quantum dots of different sizes can be excited resulting in fluorescence with minimal signal overlap (Alivisatos *et al.*, 2005).

Unlike organic fluorophores, quantum dots are highly photostable molecules and are resistant to photobleaching (Zhou and Ghosh, 2006). It has been shown that quantum dots exhibit fluorescence for up to 14 hours upon constant illumination with a 50mW, 488nm laser. In comparison, the organic fluorophore, fluorescein photobleaches completely under the same conditions in a time span of less than 20 minutes (Azzazy *et al.*, 2007). This property makes quantum dots suitable for use in assays that need to be conducted over a period of time.

Quantum dots also have a large stoke shift which is defined as the difference between the peak absorption and the peak emission wavelengths (Fu *et al.*, 2005; Gao *et al.*, 2005). This property of quantum dots makes them useful for *in vivo* imaging as quantum dots are able to overcome the auto fluorescence common in biological samples (Gao *et al.*, 2005).

Even though quantum dots clearly have better properties as dyes in comparison to organic fluorophores, they are unlikely to completely eliminate the use of organic dyes. This is partly due to the fact that quantum dots are expensive. It will also take a considerable amount of time to introduce quantum dots as primary molecules for fluorescence purposes as quantum dots have to be optimized for use (Smith and Nie, 2004).

1.7.1.2. Bioconjugation of quantum dots

Application of quantum dots in biological studies is only possible through conjugation of the quantum dots to biological molecules. These molecules include antibodies, peptides, oligonucleotides as well as aptamers (Azzazy *et al.*, 2007). Several methods are applied in the conjugation of biological molecules to quantum dots. These include adsorption, electrostatic interaction, mercapto (-SH) exchange as well as covalent linkage (Alivisatos *et al.*, 2005).

Conjugation via adsorption is usually non-specific. Small molecules such as oligonucleotides and several serum albumins have been shown to bind non-specifically to quantum dots. Adsorption is dependent on factors such as pH ionic strength, temperature as well as the surface charge of the molecules (Alivisatos *et al.*, 2005; Azzazy *et al.*, 2007).

Electrostatic interactions have also been used for the bioconjugation of biomolecules to quantum dots. This method usually employs the binding of proteins to a negatively charged quantum dots. To achieve this, a protein is engineered to fuse with a positively charged domain and this domain then binds to the quantum dot surface. This method produces stable quantum dot–protein conjugates that usually have a higher quantum yield than the unconjugated quantum dot (Alivisatos *et al.*, 2005; Azzazy *et al.*, 2007).

Biomolecules can also be conjugated to a quantum dots using mercapto exchange method. This method is useful for biomolecules that have thiol groups. These thiol groups bind to the zinc surface. Unfortunately the binding between zinc and the thiol group is usually not strong enough and as such the zinc thiol- bond can easily be broken resulting in precipitation of the quantum dots in solution (Alivisatos *et al.*, 2005).

The most stable bioconjugation between quantum dots and biomolecules is through covalent bonding using cross linking reagents. The most commonly used cross linking reagents are carbodiimides, particularly 1-ethyl-3-(3-dimethylamino) carbodiimide HCl (EDC) (Montalbetti and Falque, 2005). Several properties of carbodiimides have made them attractive for cross linking reactions. Carbodiimides are generally stable and can be stored easily. In catalytic reactions, carbodiimides are very reactive owing to saturating ability of the unsaturated C=N bond and as such they provide a powerful driving force in a reaction (William and Ibrahim, 1981). Carbodiimides are also attractive because they are zero length cross linkers. Hence the products of a chemical reaction are without residues with the advantage that a number of purification steps for the desired product are reduced (Nakajima and Ikada, 1994). The linker molecule (EDC) is used to join -NH₂ and -COOH groups that are either on the quantum dot or the biomolecule or vice versa. EDC reagent reacts with carboxylic acid group to form an active O-acylisourea intermediate. This intermediate then couples to the amino group on the peptide and an EDC by product is displaced into solution by a nucleophile. The formation of a peptide bond using EDC is illustrated in Figure 1.6.

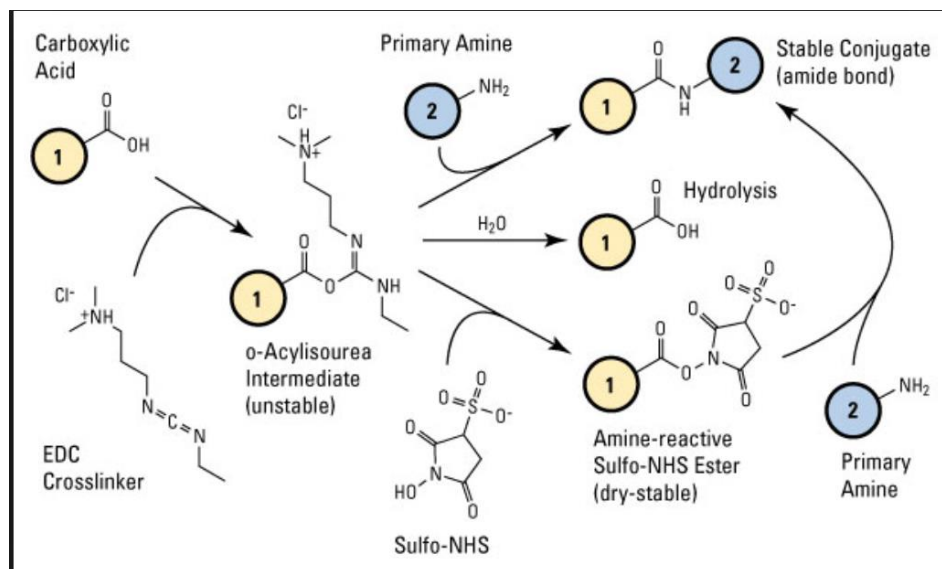


Figure 1.6: Amide bond formation. Formation of a peptide bond between a carboxyl group and an amine group using the coupling reagent EDC (<http://www.piercenet.com/products/browse.cfm?fldID=02030312>).

As previously mentioned both peptides and antibodies are used as targeting molecules in biological assays. The activity of these biomolecules can be evaluated by conjugating them to quantum dots as well as organic fluorophores.

1.8. Tumour targeting using quantum dots and peptides for Cancer Diagnosis

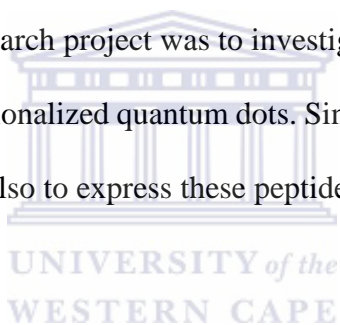
The unique optical properties of quantum dots combined with the positive attributes of peptides have presented exciting opportunities to specifically target cancer cells that can be applied in cancer diagnostics. Studies in this arena are demonstrating specific targeting of cancer cells and tumors. Haglund and others performed an experiment in which the peptide LTVSPWY was attached to quantum dots (Haglund *et al.*, 2009). The peptide quantum dot conjugates were

incubated with the breast cancer cell lines SKBR3 and MCF-7 which served as a negative control. Fluorescence was demonstrated by microscopy in both cell lines. Fluorescence was seen around the edges of the cells as well as intracellularly in SKBR3 cells. Fluorescence was not observed in the MCF-7 cells (Haglund *et al.*, 2009). This experiment paved the way for the *in vivo* demonstration of tumor cell targeting. SKBR3 cells were infused in mice to induce tumor growth. Quantum dots with the conjugated peptide LTVSPWY were intravenously infused into mice. Tumors were excised from the mice and tissue sections were prepared. Tissue preparations showed presence of quantum dots in tumor tissue. As a control kidney tissue was sectioned and fluorescence imaging of this tissue did not reveal the presence of quantum dots (Haglund *et al.*, 2009).

In another study by Guo and others, Zn-Cu-In-S/ZnS quantum dots were conjugated to cRGD peptide (Guo *et al.*, 2013). The cRGD peptide binds specifically to the $\alpha\beta_3$ integrin receptor that plays a role in metastasis and angiogenesis in many human cancers. Following conjugation the quantum dot peptide conjugate was intravenously infused in the tail vein of tumor bearing nude mice. After 30 minutes, fluorescence signals from the quantum dot peptide conjugate were detected in the tumor region. In contrast fluorescence around the tumor region was not detected in mice that were intravenously infused with quantum dots only (Guo *et al.*, 2013). The studies show how quantum-peptide dot conjugates can be applied for the diagnosis of cancer.

1.9. Objectives

Cancer is a disease that often has a fatal outcome. Survival depends on the early detection of the disease. Technologies that are used to detect biochemical changes (biomarkers) that can be associated with the disease have been instrumental in the detection of cancer and have saved many lives. Quantum dots in conjunction with cancer specific peptides are now emerging as a new tool to detect and diagnose cancer. The unique imaging properties of these nanoparticles can facilitate the production of new diagnostic systems that are more reliable and affordable than the diagnostic methods that are currently available. Although a number of cancer targeting peptides have been identified, very few of these peptide have been studied for their selectivity towards different cancer cells. Therefore the aim of this research project was to investigate the specific binding of selected peptides to cancer cells using functionalized quantum dots. Since the cost of synthetic peptides are so high, the aim of this study was also to express these peptides in *E.coli* bacterial cells.



CHAPTER 2: MATERIALS AND METHODS

2.1 Materials used and Suppliers

Materials	Suppliers
Acetic Acid	Merck
Acetone	Merck
40% acrylamide Bis Solution 37:5:1	Serva
Agarose	Whitehead Scientific
Ammonium Persulphate (APS)	Merck
Ampicillin	Fermentas
Bacteriological agar	Merck
Bovine Serum Albumin (BSA)	Roche
Bromophenol blue	Merck
Cesium Chloride	Roche
Coomassie Brilliant Blue R-250	Bio-Rad
4', 6- diamidino-2-phenylindole (DAPI)	Fermentas



Detection Solution	Thermo Scientific
Dimethyl dicarbonate	Sigma
Dithiothreitol (DTT)	Fermentas
Dulbecco's Modified Eagle's Meduim (DMEM)	Gibco/Lonza
1-Ethyl-3-(3-(dimethylamino)propyl)-carbodiimide (EDC)	Sigma
Ethylene Diamine Tetra-acetic acid (EDTA)	Merck
Ethanol	Merck Chemicals
Ethidium Bromide	Sigma
Fetal Calf Serum	Lonza
6X Gel Loading Buffer	Fermentas
Glycerol	Merck
Glycine	Merck
Hisprobe Antibody	Santa Cruz
Hydrochloric Acid	Merck
Isopropanol	Merck



Methanol	Merck
Mowiol	Sigma
Nuclease free water	Fermentas
Oligonucleotides	Inqaba biotec
Penicillin-Streptomycin	Invitrogen
Peptides	GL Biochem
pET21b Plasmid	Novagen
Potassium Acetate	Merck
Quantum dots	Invitrogen
Sodium Chloride	Merck
Sodium Dodecyl Sulphate (SDS)	Merck
Sodium Hydroxide	Merck
N,N,N',N'-Tetramethylethylenediamine (TEMED)	Sigma
Tris (Tris [hydroxymethyl] aminoethane)	Merck
Tryptone	Merck
Trypsin	Gibco



Tween 20	Merck
Urea	Sigma
Yeast Extract	Merck

2.1.1. List of kits

Extract II PCR clean gel extraction	Macheret-Nagel
QIAEX II Gel Extraction Kit	Qiagen



2.2. Solutions and Buffers

Ammonium persulphate: 10% stock was prepared in 10ml of distilled water. The solution was stored 4°C.

Ammonium acetate buffer: 10mM Ammonium acetate, pH 6

Borate Buffer: Boric acid 50mM, pH 7.5 and pH 8.5

Coomassie Brilliant blue (CBB) staining solution: 0.25% Coomassie Brilliant Blue R250, 45% methanol and 5% acetic acid

Destaining solution: 30% methanol and 10% acetic acid in distilled water

DTT buffer: 2% (w/v) Dithiothreitol (DTT) in SDS equilibration buffer.

6X Glycerol BPB Gel Loading Buffer: 30% Glucose and 0.3% Bromophenol blue.

GTE solution: 0.05M Glucose, 0.025M Tris, 0.01M EDTA.

Luria agar: 10g/l Tryptone, 5g/l Yeast Extract Powder, 5g/l NaCl, 14g/l Bacteriological Agar.

Luria Broth: 10g/l Tryptone, 5g/l Yeast Extract Powder, 5g/l NaCl. .

Phosphate buffered saline (PBS): 13mM NaCl, 2.7mM KCl, 8mM Na₂HPO₄ and 1.5mM KH₂PO₄, pH 7.4

Potassium acetate (KAc): 3M KAc in 500ml

5X sample buffer: 250mM Tris-HCl, pH 6.8, 62.5% Glycerol, 0.025% BPB, and DTT to a final concentration of 125mM.

10X SDS electrophoresis buffer: 250mM Tris, 10% SDS and 1.92M glycine, pH 8.3.

12X Separating Gel Buffer: 1.5M Tris-HCl, pH 8.8.

Sodium Chloride-saturated isopropanol: NaCl was added to isopropanol until completely saturated.

Sodium hydroxide/Sodium dodecyl sulphate (NaOH/SDS): 0.2M NaOH, 1% SDS.

4X Stacking Gel Buffer: 0.5M Tris-HCl, pH 6.8.

10X TBE: 0.9M Tris, 0.89M Boric Acid, 25mM EDTA pH 8.3. This stock solution was diluted 10 fold for electrophoresis of agarose.

TBS-Tween: 20mM Tris-HCl and 150mM NaCl, pH 7.4 and 0.1% Tween 20 (stored at 4°C).

TBS-Tween (containing 5% milk): 5% low fat dried milk powder in TBS-Tween.

TE-CsCl solution: CsCl was added to 1X TE until completely saturated.

10X TE: 0.1M Tris, 0.01M EDTA pH 7.5.

Tfb1 buffer: 30mM potassium acetate, 50mM MnCl₂, 0.1M KCL, 6.7mM CaCl₂ and 15% glycerol (v/v).

Tfb 2 buffer: 10mM Na-MOPS, 10mM KCl, 75mM CaCl₂, 15% (w/v) glycerol, pH 7.0

Transfer Buffer: 25mM Tris, 192mM glycine and 20% methanol (stored at 4°C).

2.3. Design of oligonucleotides for the expression of peptides

Cancer targeting peptides (Table 2.1) were identified from the literature (Shadidi and Sioud, 2003).

The peptide sequences were translated into nucleotide sequences. The peptide oligonucleotides were designed to include *XhoI* and *NdeI* restriction sites. The *XhoI* site was included in the anti-sense strand and the *NdeI* restriction was included in the sense strand of the oligonucleotides.

Oligonucleotides were designed for cloning into the pET21b plasmid digested with *XhoI* and *NdeI*.

The oligonucleotides were obtained from Inqaba Biotec.

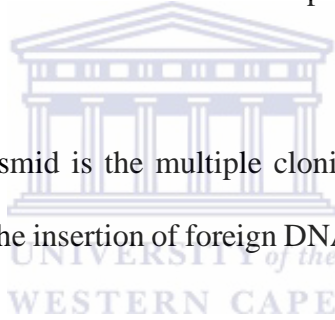
Table 2.1. Peptide sequences and oligonucleotide sequences

Peptide name	Peptide sequence	Oligonucleotide sequence
p6.1	KCCYSL	Sense 5' T ATG AAA TGT TGT TAT TCT CTT C 3' Anti-sense 5' TCGAG AAG AGA ATA ACA ACA TTT CA 3'
p.L	LTVSPWY	Sence 5' TATG CTG ACC GTG AGC CCG TGG TAT C 3' Anti-sence 5' TCGAG ATA CCA CGG GCT CAC GGT CAG CA 3'
NL1.1	MYWGDSHWLQYWE	Sense 5' TATG TAT TGG GGT GAT TCT CAT TGG CTT CAA TAT TGG TAT GAA C 3' Anti-sense 5' TCGAG TTC ATA CCA ATA TTG AAG CCA ATG AGA ATC ACC CCA ATA CA 3'
MV	SLWDQGNFPLGGGC	Sense 5' T ATG TCT CTG TGG GAT CAG GGC AAC TTT CCG CTG GGT GGT GGT TGC C 3' Anti-sense 5' TCGAG GCA ACC ACC ACC CAG CGG AAA GTT GCC CTG ATC CCA CAG AGA CA 3'

2.3.2 Cloning vector

The features of pET21b plasmid include a T7 viral promoter that is highly selective for T7 RNA polymerase and the Lac I repressor which encodes a repressor protein that prevents expression from the T7 Lac promoter. The Lac I repressor is vital as it prevents expression of protein that could be potentially toxic to the bacterial host and consequently transformation efficiency of the bacterial host is increased. Other features include the origin of replication at which DNA replication is initiated, an f1 origin of replication which allows for single stranded replication of the vector when co infected with M13 helper phage and an ampicillin resistance gene which offers selectivity by enabling only bacterial hosts that have the plasmid to grow in media containing ampicillin.

Another composite part of the plasmid is the multiple cloning site or polylinker which houses unique restriction sites that enable the insertion of foreign DNA resulting in a recombinant product (Novagen, 2003).



2.4. Preparation of pET21b DNA

2.4.1. Preparation of pET21b plasmid using cesium chloride/ethidium bromide fractionation

10ml of a saturated culture of plasmid-containing *E. coli* containing pET21b plasmid was diluted into 1000ml 2X TY broth containing the appropriate antibiotic and grown for 16 hours with shaking at 37°C. The bacteria were pelleted by centrifugation at 4 500g for 10 minutes at 4°C. The pellet was resuspended in 4ml GTE and incubated on ice for 10 minutes. The cells were lysed by the addition of 8ml NaOH/SDS with gentle swirling and incubated on ice for 10 minutes. 6ml of 3:5M KOAc was added and mixed gently to neutralize the alkali, and the mixture incubated on ice for 10 minutes. The precipitate of cell debris, chromosomal DNA and SDS was removed by centrifugation at 4 500g for 15 minutes at 4°C. The supernatant was filtered through glass wool to remove particulate material and the nucleic acids precipitated by the addition of 0.8 volumes propan-2-ol, followed by incubation at -20°C for 20 minutes. The precipitate was pelleted by centrifugation at 10 000g for 10 minutes at 4°C. Plasmid DNA was separated from RNA by double CsCl/ethidium bromide fractionation.

The propan-2-ol pellet was resuspended in 4.5ml of TE. The solution was mixed with 4mg ethidium bromide and 5.75g CsCl to give a final density of 1.61g/ml. This mixture was centrifuged at 10 000g for 10 minutes at 20°C. The pellet was mainly RNA. The supernatant was transferred to Quickseal tubes and centrifuged at 55 000g for 18 hours at 20°C in NVi 65 rotor. The plasmid DNA was visualized with a 360nm UV illuminator and recovered using a syringe and made up to 5ml with TE/CsCl and ethidium bromide to give a final density of 1.61g/ml. This mixture was transferred to a clean Quickseal tube and centrifuged at 55 000g for 18 hours at 20°C in NVi 65 rotor.

The plasmid DNA was again recovered and an equal volume of NaCl-saturated isopropan-2-ol was added to remove the ethidium bromide. This extraction was repeated four times. Two volumes of water and one volume of isopropan-2-ol were added to precipitate the DNA. This mixture was mixed well and incubated on ice for 10 minutes. The DNA was recovered by centrifugation at 10 000g for 15 minutes. The pellet was resuspended in TE at 1mg/ml and stored at 4°C (short term) or -20°C (long term).

2.4.2. Restriction digestion of pET21b plasmid

An amount of 1µg of pET21b plasmid digested with *XhoI* restriction enzyme for 1 hour at 37°C according to Table 2.2. The digested plasmid was then run on an agarose gel and excised from the gel. The plasmid was extracted from the gel using the nucleospin extract II according to manufactures instructions. The total volume of the extracted plasmid digested with *XhoI* was 50µl. The extracted plasmid was the digested with *NdeI* enzyme for 1 hour at 37°C to ensure complete digestion. The digest was then run on an agarose gel and excised from the gel. The plasmid was extracted using nucleospin extract II. The final concentration of the gel purified plasmid was 64.4ng/µl as determined by nanodrop 1000 spectrophotometer.

Table 2.2 Reagents used to digest pET21b Plasmid using *XhoI*

Reagents	Volume
Plasmid(1μg)	25 μ l
Enzyme (10X)	1 μ l
Buffer (10x)	10 μ l
Nuclease free water	64 μ l

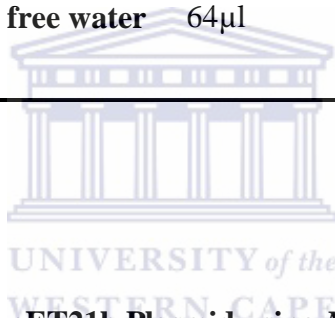


Table 2.3 Reagents used to digest pET21b Plasmid using *NdeI*

Reagents	Volume
Plasmid (1μg)	50 μ l
Enzyme (10X)	1 μ l
Buffer (10X)	10 μ l
Nuclease free water	39 μ l

2.4.3. Agarose gel electrophoresis of DNA

DNA was electrophoresed on a 1% agarose gel. The agarose was made by the addition of the appropriate amount of agarose to 1X TBE and boiling the solution until dissolved, followed by the cooling of the agarose and the addition of ethidium bromide to a final concentration of 1µg/ml. The agarose was poured into gel casting trays and allowed to solidify. DNA was mixed with an appropriate amount of gel loading buffer. The gels were electrophoresed at 100 V in 1X TBE electrophoresis buffer. After electrophoresis, the gels were viewed with the use of UV trans-illuminator. Gel images were captured with an image capture system (Kodak Digital Science ID).

2.4.4. Gel purification of DNA



The DNA was electrophoresed on a 1% agarose gel in 1X TBE (Section 2.4.3). The DNA was viewed with the use of long wavelength (360nm) UV lamp. The DNA fragment of interest was cut out with a sterile blade. The PureLink™ Quick Gel Extraction Kit from Invitrogen was used according to the manufacturer's instructions. The gel slice which contained the DNA fragment was weighed in a 5ml tube. To the latter, 6 volumes of gel solubilization buffer (L3) for every 400mg of gel was added to the gel slice. The tubes which contained the gel slice and solubilization Buffer were placed in a 50°C heating block for 10 minutes. The tubes were inverted every 3 minutes to ensure gel dissolution. The gel slice was incubated for a further 5 minutes. The dissolved gel slice containing the fragment of interest was pipetted into the centre of a PureLink™ Clean-up Column, inserted in a wash tube.

The column was centrifuged at 10 000g for 1 minute. The flow-through was discarded and the PureLink™ Spin Column was reinserted into the wash column. An amount of 700µl of wash buffer was added to the PureLink™ Spin Column. The column was centrifuged at 16 000g for 2-3 minutes to remove any residual wash buffer and ethanol. The wash tube was discarded and the PureLink™ Spin Column was placed into a sterile elution tube. An amount of 50µl elution buffer was added to the centre of the PureLink™ Spin Column and incubated for 1 minute at room temperature. The column was centrifuged at 10, 000g for 1 minute to elute purified DNA. The PureLink Spin Column was discarded and the flow through containing purified DNA was stored at – 20°C.



2.5. Strains

The bacterial strains used for protein expression are shown in Table 2.4

Table 2.4 Bacterial strains used

Name	Genotype
<i>E. coli</i> Arctic Express(DE3) pLysS	F ⁻ <i>ompT hsdS</i> (rB ⁻ mB ⁻) dcm ⁺ Tetr gal λ(DE3) <i>endA</i> Hte [<i>cpn10cpn60</i> Gentr], <i>pLysS</i> , Cm ^R
<i>E. coli</i> BL21 DE3	F ⁻ <i>ompT gal dcm lon hsdSB</i> (rB ⁻ mB ⁻) λ(DE3 [<i>lacI</i> <i>lacUV5-T7 gene 1 ind1 sam7 nin5</i>])
<i>E. coli</i> BL21-CodonPlus (DE3)-RIL	F ⁻ <i>ompT hsdS</i> (rB ⁻ mB ⁻) dcm ⁺ Tetr gal λ(DE3) <i>endA</i> Hte [<i>argU ileY leuW</i> CmR]
<i>E. coli</i> MC1061	MC1061 F ⁻ , <i>araD139</i> , (<i>ara leu</i>)7697, Δ <i>lacX74</i> , <i>galU</i> ⁻ , <i>galK</i> ⁻ , <i>hsr</i> ⁻ , <i>hsm</i> ⁺ , <i>strA</i>

2.6. Preparation of competent *E. coli* cells

The bacterial strains used were MC1061 and BL21 (DE3) cells. These were streaked on an LB agar plate containing 10mM MgCl₂. A single colony from this plate was used to inoculate 20ml TYM Broth. The culture was incubated at 37°C until an optical density (OD) of 0.2 at 550nm was reached. The culture was transferred into a 2l flask, 400ml TYM broth was added and the culture was incubated at 37°C until the optical density at 550nm was between 0.4 and 0.6. The culture was

cooled rapidly in ice water and centrifuged at 6000g for 10 minutes at 4°C in a Beckman J2-21 centrifuge. The supernatant was discarded and the cell pellet re-suspended in 250ml ice-cold Tfb1 buffer. After 30 minutes the cell suspension was centrifuged at 6000g for 10 minutes at 4°C. The pellet was gently re-suspended in 50ml Tfb 2 buffer and dispensed in 300µl aliquots and then rapidly frozen using liquid nitrogen. These aliquots were stored at -80°C.

2.7. Cloning of oligonucleotides

2.7.1. Annealing of oligonucleotides

The sense and antisense oligonucleotides were purchased from Inqaba Biotec. The oligonucleotides were re-suspended in nuclease free water and the concentrations of the oligonucleotides were determined using the nanodrop. The oligonucleotides were heated at 95°C for 5 minutes and then allowed to anneal at room temperature overnight. The final concentrations were 0.2µg/ul.

2.7.2. Ligation of oligonucleotides into pET21b plasmid

The ligation reaction was set up based on the following equation:

$$\frac{\text{Amount of vector (ng)} \times \text{size of insert (kb)} \times \text{Insert: Vector ratio}}{\text{Size of vector (kb)}} = \text{ng}$$

Table 2.5 Reagents utilized in the ligation reactions of oligonucleotide encoding p.L

Reagents	Vector insert ratio	
	10:1	20:1
	Volumes	
Oligonucleotide(431.4 ng/μl)	1 μl	1.5 μl
pET21b(10ng)	1 μl	1 μl
Buffer(10X)	1 μl	1 μl
T4 DNA ligase(U/μl)	1 μl	1 μl
Nuclease free water	6 μl	5.5 μl
Total	10 μl	10 μl



Table 2.6 Reagents utilized in the ligation reactions of oligonucleotide encoding p6.1

Reagents	Vector insert ratio	
	10:1	20:1
	Volumes	
Oligonucleotide (422.8ng/μl)	1 μ l	1 μ l
pET21b (10ng)	1 μ l	1.5 μ l
Buffer (10X)	1 μ l	1 μ l
T4 DNA ligase (U/μl)	1 μ l	1 μ l
Nuclease free water	6 μ l	5.5 μ l
Total	10 μ l	10 μ l



Table 2.7 Reagents utilized in the ligation reactions of oligonucleotide encoding MV

Reagents	Vector insert ratio	
	10:1	20:1
	Volumes	
Oligonucleotide (489.6ng/μl)	1.34μl	2.64μl
pET21b (10ng)	1μl	1μl
Buffer (10X)	1μl	1μl
T4 DNA ligase (U/μl)	1μl	1μl
Nuclease free water	5.7μl	4.36μl
Total	10μl	10μl



Table 2.8 Reagents utilized in the ligation reactions of oligonucleotide encoding NL1.1

Reagents	Vector insert ratio	
	10/1	20/1
	Volumes	
Oligonucleotide(180.5ng/μl)	1μl	1.64μl
pET21b(10ng)	2μl	2μl
Buffer (10X)	1μl	1μl
T4 DNA ligase(U/μl)	1μl	1μl
Nuclease free water	5μl	4.36μl
Total	10μl	10μl

The ligation mixtures were incubated overnight at 4°C to allow ligation to occur.

2.7.3. Transformation

Competent MC1061 cells (100µl) were added to the ligated reagents and the preparations were placed on ice for 20 minutes. This was followed by heat-shocking for 1 minute at 42°C without shaking and the preparations were placed on ice for five minutes. To the mixtures, 900µl of Luria bertani (LB) media was added and incubated at 37°C for 1 hour with shaking. Thereafter an amount of 50 – 200 µl of bacterial culture was plated on pre-warmed LB agar plate and incubated at 37°C overnight.

2.7.4. Screening of positive colonies

Following transformation, four colonies were selected from the plates and cultured in 10ml of LB media overnight at 37°C. After culture, glycerol stocks were prepared and bacteria were streaked on LB agar ampicillin plates. The plates were sent to Inqaba biotec for sequence analysis. Plasmid DNA was analyzed using universal primers.

2.8. Protein expression

The pET21b plasmids containing the inserts were transformed in BL21 (DE3) expression hosts. Bacteria were then cultured in 100ml of Luria broth at 37°C overnight. Following culture 900ml Luria broth was added and the optical density was determined at 550nm using a Thermo spectronic Helios spectrophotometer (Thermo Scientific). The bacteria were cultured at 37°C until and optical density reading of between 0.4 and 0.6 was obtained. Protein expression was induced with 1mM

IPTG. Prior to induction 1ml of un-induced sample was collected. The cells were grown at 25°C overnight. Following culture the cells were centrifuged at 10 000g for 10 minutes using a sorval RC6 Centrifuge (Thermal Electron Corporation). The supernatant was returned for analysis as described in section 2.8.1. Lysis buffer (1X PBS, 100µg/ml lysozyme and protease inhibitor) was added to the cell pellet. The cells were lysed using a sonicator. Following lysis the cells were centrifuged at 16 000g for 30 minutes and the supernatant was collected and stored at -20°C. The samples were prepared by adding 10µl of sample buffer to 20µl of lysate. These were electrophoresed by SDS-PAGE.

2.8.1. Protein precipitation

Following transformation in MC1061, BL21(DE3), BL21 CodonPlus and Arctic express cells, bacteria were cultured and induced with 1mM IPTG and grown overnight at 25°C and 10°C for arctic express cells. The cultures were then centrifuged at to obtain the supernatant at 10 000g using a sorval RC6 (Thermal Electron Corporation) for 10 minutes. Following centrifugation 5 volumes of ice cold acetone was added to 1 volume of supernatant and this was stored at -20°C overnight. The precipitated proteins were then centrifuged and the supernatant was discarded. The pellet was air dried at room temperature and then suspended in PBS buffer containing 1mM DTT, 0.5% triton X-100 and protease inhibitor. The proteins were kept on ice for an hour and then centrifuged at 10 000g using bench top centrifuge. The pellet was resuspended in 20µl sample buffer. The resuspension was boiled at 95°C for 5 minutes and 10µl of the sample was loaded on SDS-page gels.

2.9. 1D SDS-Polyacrylamide Gel Electrophoresis

2.9.1. Gel preparation

The proteins were separated by 1D polyacrylamide gel electrophoresis. Glass plates and apparatus (Biorad) used were first cleaned to ensure that they were free of acrylamide. The gel plates were set up in the gel casting apparatus (Biorad). An 18% separating gel solution was prepared according to Table 2.9. The separating solution was poured in between the two plates and overlaid with 1ml isopropanol and allowed to solidify.

Table 2.9 Stock solutions for the 18% Separating gel solution

Reagents	18% Gels
Separating Buffer (1.875M Tris-HCl, pH8.8)	2ml
40% Acrylamide-Bis (37:5:1)	4.5ml
10% SDS	100µl
10% APS	50µl
Distilled water	3.34ml
TEMED	10µl
Total Volume	10ml

The stacking gel solution was prepared according to Table 2.10. Once the separating solution was solidified the isopropanol was poured off and the gel was rinsed thoroughly with distilled water. The stacking solution was poured in between the gel plates and a 10 well Biorad comb was inserted into the stacking gel. The gel was allowed to solidify. The comb was removed and the gel was set up in the Gel electrophoresis tank (Biorad). The tank was filled with 1X SDS electrophoresis buffer and was electrophoresed at 80V for 5 minutes to remove residual SDS or acrylamide from the wells.

Table 2.10: Stock solutions for the 4% stacking gel solution

Reagents	4% Gels
Stacking Buffer (0.625M Tris-HCl, pH6.8)	1ml
40% Acrylamide-Bis (37:5:1)	1ml
10% SDS	100µl
10% APS	75µl
Distilled water	8ml
TEMED	20µl
Total volume	10ml

2.9.2 Sample preparation and gel loading

The protein samples were removed from -20°C and thawed immediately. In a 1.5ml tube, 30µl of the protein sample was added to 10µl of 5X sample buffer. The samples were centrifuged for 5 minutes at 16000g using bench top Eppendorf centrifuge. The protein samples were boiled for 5 minutes at 95°C. The samples were loaded onto the polyacrylamide gel and were electrophoresed at 100V until the coomassie dye reached the bottom of the gel.

2.9.3. Gel staining

The gel was removed from the gel plates and stained in Coomassie staining solution for 45 minutes on a shaker. The staining solution was removed and the gel was destained for 10 to 16 hours whilst shaking in destaining solution.



2.10. Western blot

2.10.1 Blot transfer of proteins onto PVDF membrane

The proteins were analyzed by 1D SDS polyacrylamide gel electrophoresis according to section 2.9. After electrophoresis the proteins were transferred onto the PVDF membrane (Biotrace) by blot transfer using a transfer blot apparatus. The blot apparatus was set in the running tank filled with ice cold transfer buffer and the proteins were electroblotted for 90 minutes at 110 V.

2.10.2 Western plot analysis of peptides.

The membrane was blocked in 5% milk TBS-Tween for 1 hour at room temperature. After 1 hour the membrane was washed with TBS-Tween and the primary antibody (His-probe) was diluted in 3% BSA and incubated at 4°C overnight. The his-probe was used to detect the histidine tag present on the peptide. The membrane was washed in TBS-Tween for 5 minutes at room temperature with shaking 3 times. The membrane was then incubated with 4ml (1:1) Super Signal West Pico Working solution (Thermo Scientific) for 5 minutes in the dark. The positive control used was a 25kDa protein from InlC from *Listeria monocytogenes* kindly donated by Lilia Poole (University of Western Cape).



UNIVERSITY of the
WESTERN CAPE

2.10.3. Development of the film.

A CL-Xposure film (Thermo Scientific) was exposed to the blot for 1 and 5 minutes. After the exposure of the film, the film was developed in a Cunix 60 X-ray developer (AFGA). The UVP Biospectrum imaging system (UVP, LCC) was also used to analyse membranes.

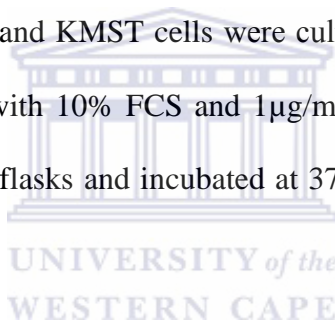
2.11. Cell culture

2.11.1. Cell lines

A panel of cell lines were used. These included human epithelial colorectal adenocarcinoma cells (CACO-2), cervical cancer cells (HELA), human hepatocellular liver carcinoma (HEPG2), osteoadenocarcinoma (HT29) and human fibroblast cell line (KMST-6).

2.11.2. Cell propagation

CACO-2, HELA, HEPG2, HT-29 and KMST cells were cultured in Dulbecco's modified eagle medium (DMEM) supplemented with 10% FCS and 1µg/ml penicillin-streptomycin. The cells were propagated in 25cm² culture flasks and incubated at 37°C for 24-48 hours in an incubator supplied with 5% carbon dioxide.



2.11.3 Trypsinization

The cells were detached from the base of the culture flasks enzymatically using trypsin. The media was removed from the flasks and the cells were washed with PBS. Trypsin (0.125%) was added to the cells and the cells were incubated for 5 minutes. The enzymatic action of trypsin was halted by addition of DMEM. The cells were transferred to a 15ml centrifuge tube and collected by centrifugation at 3000g for 3 minutes using a Sorvall TC centrifuge (Thermo Electron Corporation).

2.12. Peptide design

Table 2.11 shows the peptides used for conjugation to Qdot 525 carboxyl nanocrystals. The peptides were designed with a terminal amine group for formation of an amide bond with the carboxyl groups on the quantum dot.

Table 2.11 Sequences of chemically synthesized peptides

Peptide name	Peptide sequence
p.C	CVFSSSYSSSC-NH ₂
Frop1	EDYELMDLLAYL-NH ₂
p.H	HEWSYLAPYPWF-NH ₂
p6.1	KCCYSL-NH ₂
P.L	LTVSPWY-NH ₂

The peptides were synthesised by GL Biochem (Shanghai, China)

2.13. Qdot 525 carboxyl nanocrystal conjugation

Qdot 525 carboxyl nanocrystal (0.25 μM) was transferred to a glass vial and diluted in 1ml borate buffer at pH 7.5. The carboxyl groups on nanocrystals were activated by the addition of 50 μM EDC. An appropriate amount of peptide was added to the reaction mixture as shown in Table

2.12. The coupling ratio of the Qdot to EDC to peptide was 1: 1.5: 250. The reaction mixture was incubated at room temperature for 3 hours with gentle mixing on a shaker (Hermanson, 2008).

Table 2.12 Reagents utilized for biomolecule conjugation to Qdot 525

Reagent	Qdot	EDC	p.C	Frop-1	p.H	P6.1	p.L
Concentration	0.25 μ M	50 μ M	7.6mM	5.7mM	6.3mM	10.3mM	11.5mM
Amount(μl)	62.5	13	3.3	4.4	4	2.4	2.2



2.13.1. Conjugated nanocrystal purification

The conjugated nanocrystals were purified to remove EDC by gravity column chromatography using PD-10 desalting columns. The columns were filled with equilibration buffer (borate buffer pH 8.5). The equilibration buffer was allowed to enter the packed bed completely. This process was repeated four times and the flow through was discarded. The conjugated nanocrystals were added to the desalting column. The nanocrystals were allowed to fill the packed bed completely and the remainder of the equilibration buffer was collected and discarded. The conjugated nanocrystals were eluted in 4ml borate buffer.

2.14. Cell staining

2.14.1. Preparation of cells for analysis by fluorescence microscopy

Cells were cultured on cover slips in a six well plates and incubated for 24-48 hours at 37°C and 5% carbon dioxide. Media was removed from the plates and the cells were washed with PBS. Cells were fixed for 20 minutes using 4% paraformaldehyde. The cells were washed with PBS and incubated with conjugated (Qdot 525 nanocrystal with peptide) and unconjugated (Qdot 595 nanocrystal only) for 1 hour at room temperature. Following incubation the cells were washed twice in PBS. The cells were mounted on microscope slides using fluoroshield (Sigma).

2.14.2. Microscopy analysis

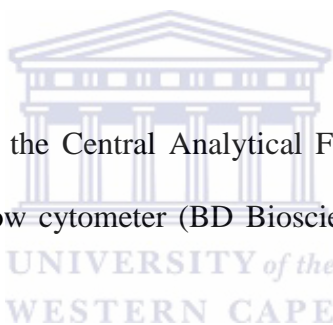
The Axioplan II fluorescence microscope (Zeiss) was used for the detection of fluorescence. The cells were stained with diamidino-2-phenylindole (DAPI) and Qdot 525 (conjugated and unconjugated). DAPI stain excites at 358nm and emits at 463nm. Therefore a long pass filter set 02 (Zeiss) designated DAPI filter was used to detect emission. The filter set 02 can detect emission of fluorescence between 365nm and 420nm. The filter set 10 (Zeiss) designated Qdot-525, was used to detect fluorescence emission spectrum of Qdot 525. The quantum dot's excitation spectra is at 415-455nm and fluorescence can be detected at 518-533nm. Cells were viewed and images were captured using 40× objective.

2.14.3 Preparation of cells for Flow cytometry analysis

Cells for Flow cytometry analysis were cultured in 24 well plates at 37°C. The cells were then removed from the plates enzymatically using trypsin. Cells were then washed with PBS and collected by centrifugation at 3000g for 5 minutes using a Sorvall TC centrifuge. The cells were fixed for 20 minutes in 4% Paraformaldehyde and then washed with PBS. The cells were stained with the Qdot 525, conjugated and unconjugated. Following 1 hour incubation at room temperature, the cells were washed with PBS. The cells were resuspended in PBS and analyzed by flow cytometry.

2.14.4. Flow cytometry analysis

Flow cytometry was performed at the Central Analytical Facility, Imaging Unit, Stellenbosch University. The BD FACSAria flow cytometer (BD Biosciences, USA) was employed for the analysis of samples.



2.14.4.1. Flow Cytometry Acquisition

Before acquisition, the sample tubes were resuspended by vortexing for 3 seconds. The FSC and SSC gain was set up in dot plot using the unstained control sample for each cell type. To set the gain of the fluorescent channel, unstained control sample was used to set the negative cells between the 1st and 2nd decade of the histogram dot plot. This setting was employed for each cell type. This enabled differentiation of the negative and high positive cells. The primary gating strategy (FSC vs SSC) was drawn to set a parent gate (P1) in order to include all cells and exclude debris. Using the P1 population, a histogram plot was used to display the intensity of the Qdot 525 fluorescence.

A secondary gate (P2) was positioned to include all the cells in that plot. After setup, the experimental samples and cell controls were acquired on the BD FACSAria. For sample acquisition, a maximum of 10 000 gated events (using P1 gate) were collected for each sample. For each sample, the Geometric median fluorescence intensity (GMFI) was used to determine the intensity of the marker fluorescence.



CHAPTER 3: RESULTS

3.1. Cloning oligonucleotides into an expression vector

3.1.1. Introduction

Cancer targeting peptides have been identified by technologies such as phage display and combinatorial chemistry. These peptides have diagnostic and therapeutic potential. However for these peptides to have clinical application they need to be produced in sufficient quantity. Recombinant DNA technology can be used to synthesize peptides in sufficient quantity at less cost in comparison to chemical synthesis. Using this technology, oligonucleotides encoding cancer targeting peptide sequence can be designed and cloned into an appropriate expression vector and subsequently expressed in a suitable host. The aim of this section was to design and cloning of oligonucleotides encoding cancer targeting peptides into pET21b plasmid vector.

Eight cancer targeting peptides were identified from the literature (Shadidi and Sioud, 2003). Oligonucleotides were designed from the amino acid sequences for the peptides. Only four oligonucleotides encoding p6.1, p.L, NL1.1 and MV were successfully cloned. The oligonucleotide design and cloning strategy adopted for the expression of the peptides is exemplified by p6.1 (KCCYSL) and shown in Figure 3.1. The same cloning strategy was used for all the peptides. An *NdeI* restriction site was incorporated downstream of the T7 promoter followed by the peptide coding sequence. An *XhoI* restriction site was added at the C terminal upstream of the histidine tag to enable incorporation of this tag to the peptide coding sequence. The pET21b vector was linearized using *NdeI* and *XhoI* restriction enzymes, thus creating overhangs that allowed for ligation with the oligonucleotide.

Peptide sequence → K C C Y S L
 DNA sequence → 5'aaa tgt tgt tat tct ctt3'
 3'ttt aca aca ata aga gaa5'

5' **tatg** aaa tgt tgt tat tct ctt **c** 3'
 3' **ac** ttt aca aca ata aga gaa **gagct** 5'

KCC coding sequence

Ligation

Vector

5' T 7 Lac promoter
 3' ca gta t

tcgag His-Tag 3'
 c 5'



DNA ligated into vector

T 7 Lac promoter KCC coding sequence His-Tag

Figure 3.1: Cloning strategy for p6.1 peptide. Oligonucleotides encoding p6.1 peptide were cloned into the *NdeI* and *XhoI* restriction sites (indicated in blue and red, respectively) of the pET21b plasmid. The oligonucleotides were designed to include the *NdeI* restriction site and *XhoI* restriction site shown in blue and red on the DNA sequence. The oligonucleotide and vector were then ligated using T4 DNA ligase.

3.1.2. Preparation of pET21b plasmid DNA

pET21b plasmid DNA was isolated using cesium chloride fractionation as described in section 2.4.1. The successful preparation of pET21b plasmid is indicated in Figure 3.2. The figure shows three bands representing nicked, linear and supercoiled plasmid.

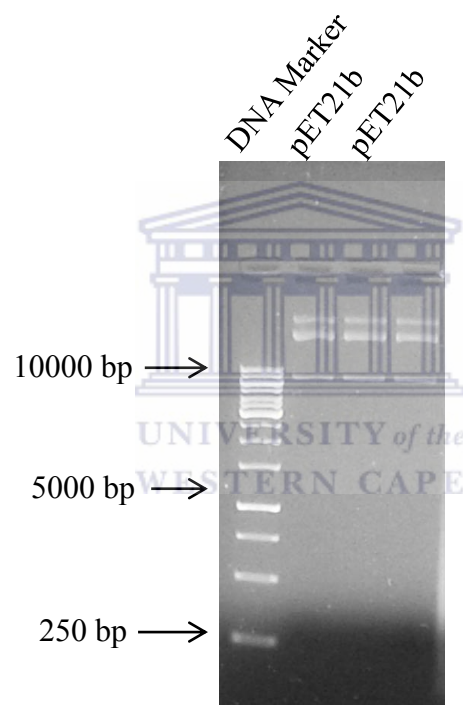


Figure 3.2: Gel electrophoresis of pET21b plasmid. The plasmid was prepared using Cesium chloride/ ethidium bromide fractionation.

3.1.3. Restriction digestion of pET21b plasmid DNA

pET21b plasmid DNA was digested using *NdeI* and *XhoI* restriction enzymes to enable ligation of the peptide coding oligonucleotides into the plasmid as illustrated in Figure 3.1. pET21b was digested using *XhoI* and *NdeI* restriction enzyme as described in section 2.4.2-2.4.4. Figure 3.3 shows digestion of pET21b plasmid DNA. A single band can be observed for the digested plasmid DNA while the uncut plasmid shows two bands.

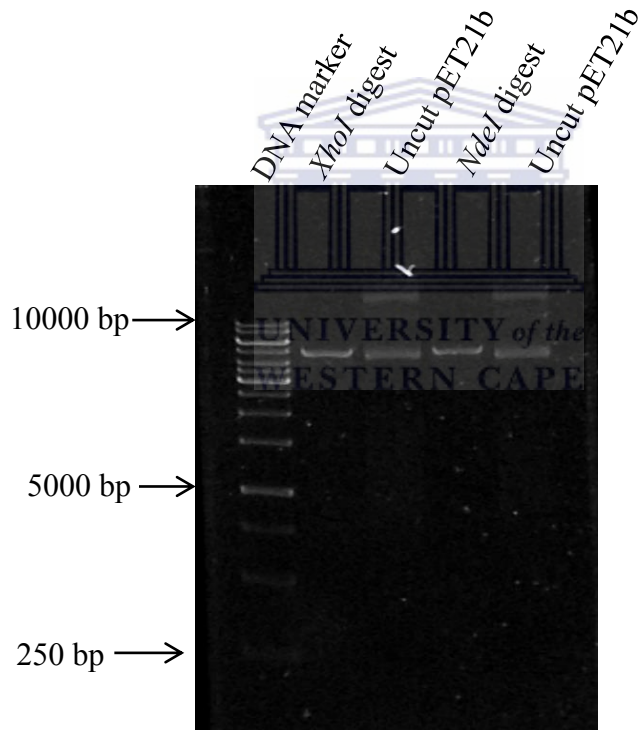


Figure 3.3: Agarose gel electrophoresis restriction digestion of pET21b. pET21b was digested using the restriction digestion enzymes *XhoI*, and *NdeI*.

3.1.4. Ligation of oligonucleotides encoding peptides into pET21b plasmid

Annealed oligonucleotides were ligated into the pET21b vector as described in section 2.7.1 and 2.7.2. Two vector insert ratios (10:1 and 20:1) were used for each peptide. The ligation reaction used to transform MC1061 *E. coli* cells is described in section 2.7.3. Table 3.1 shows the number of colonies obtained for the different oligonucleotides using the 10:1 vector insert ratio.

Table 3.1: Number of colonies obtained following transformation of Escherichia coli cells with pET21b containing oligonucleotides.

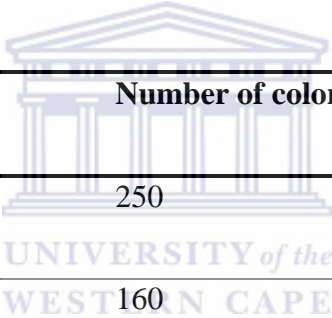


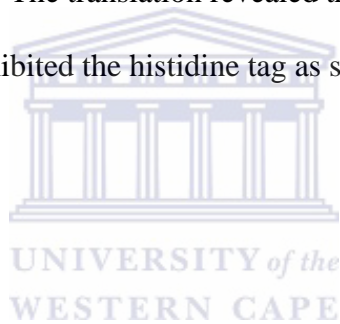
Plate	Number of colonies
p6.1	250
p.L	160
p.MV	88
NL1.1	10

3.1.5. Screening for positive clones

Screening for positive clones was done as described in section 2.7.4.

3.1.6. Sequence analysis of positive clones

T7 promoter primer and T7 terminator primer were used as sequencing primers for the forward and reverse sequencing respectively. Chromas lite version 201 was used to analyze the sequencing results received from Inqaba biotec. The FASTA format of the nucleotide sequence was obtained and ExPASy translate tool (<http://web.expasy.org/translate/>), was used to translate the DNA sequence into the protein sequence. The translation revealed the correct sequence of the p6.1, p.L, MV and NL1.1 peptides which exhibited the histidine tag as shown in Figure 3.4.



3'5' Frame

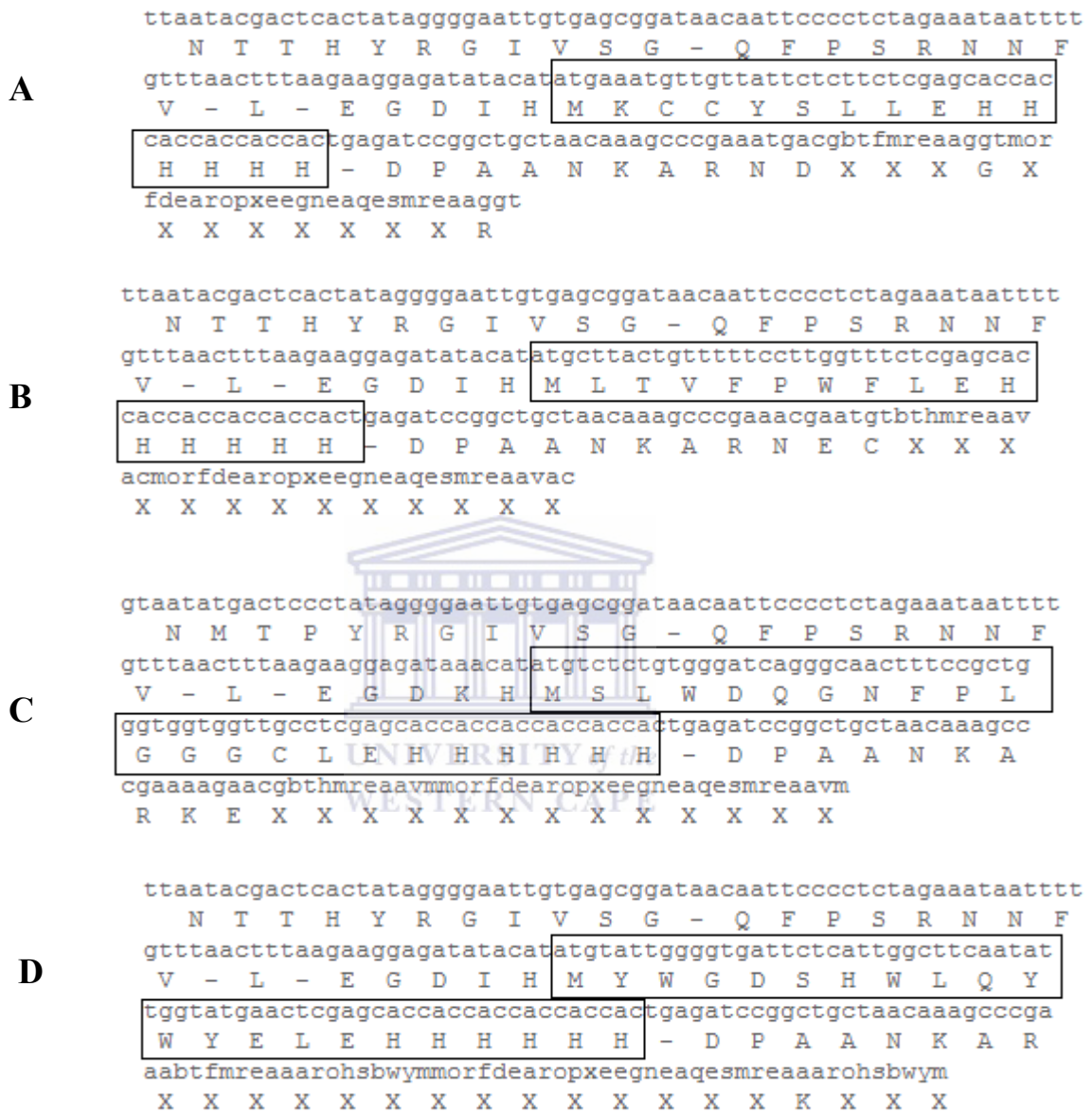
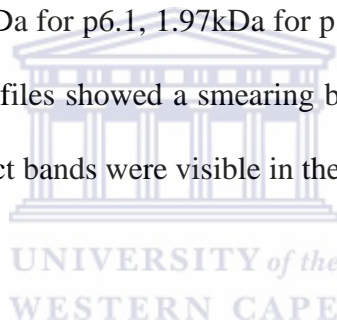


Figure 3.4: Translation of DNA sequences into protein sequences. The longest open reading frame generated by ExPASy is shown for all the peptides. A shows p6.1 sequence B shows p.L, C shows MV and D shows NL1.1. The histidine tag is shown in the sequences.

3.2.2. Expression screen of positive clones

Following confirmation of successful cloning of the oligonucleotides as indicated by the sequencing results, the next phase was to investigate if the clones express the cancer targeting peptides. This was achieved by transforming the established recombinant plasmids in an expression host namely *E.coli* B121 (DE3). The transformation reaction is described in section 2.7.3.

Expression screen was conducted as described in section 2.8. Figures 3.5 A, B, C and D show the protein expression profiles for the induced and uninduced bacterial lysate. The expected sizes of the expressed peptides were 1.78kDa for p6.1, 1.97kDa for p.L, 2.52kDa for MV and 3.3kDa for NL1.1. The protein expression profiles showed a smearing below the 10kDa marker in both the un-induced and induced. No distinct bands were visible in the region of 1.7-3.3kDa.



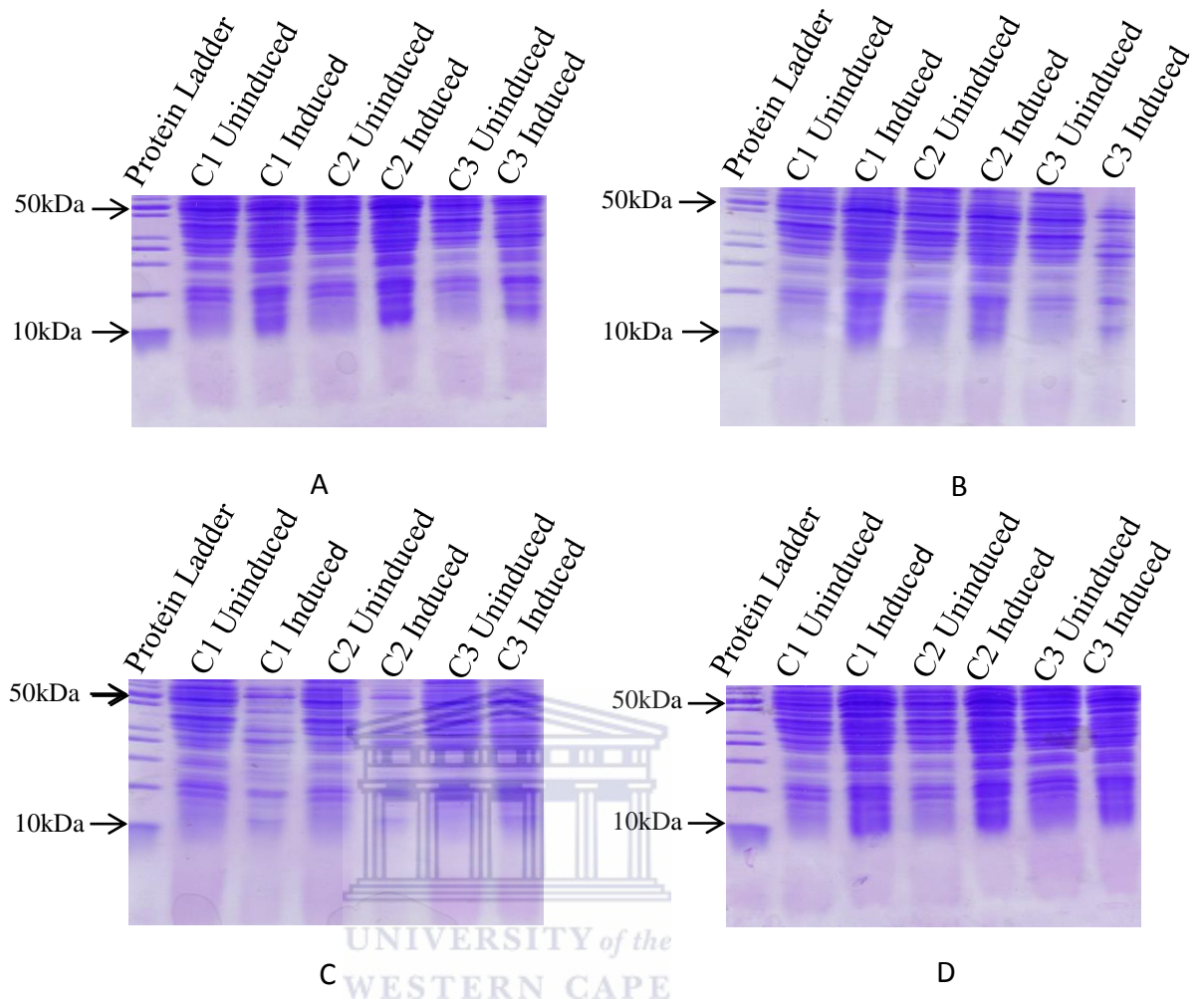


Figure 3.5: SDS PAGE of bacterial lysates. BL21 (DE3) *E. coli* cells were transformed with pET21b peptide containing sequences encoding the peptides. A shows expression screen of p6.1 peptide, B shows screening of p.L peptide, C shows screening of MV peptide and D shows screening of NL1.1 peptide. Three colonies were selected for each peptide (C1-C3). The bacteria was induced using 1mM IPTG. The expression profile was resolved on an 18% SDS polyacrylamide gel.

3.2.2.1 Screening for the presence of peptides by Western blot analysis

Screening for the presence of peptides in the lysates of bacterial cultures induced with IPTG failed to confirm the presence of the peptides. It is likely that the expression of the peptides were very low. For this reason the lysates were also probed by western blot analysis for the presence of the histidine tagged peptides. The total protein lysates of uninduced and induced bacterial cells were probed with anti-histidine antibody. The samples used in western blot analysis were the same as those used in the expression screen. The positive control used was a 25kDa histidine tagged InlC protein from *Listeria monocytogenes* and it was visible on the blot. However, no distinct bands were visible in the region of 1.7 -3.3kDa as shown in Figures 3.6 A, B, C and D.



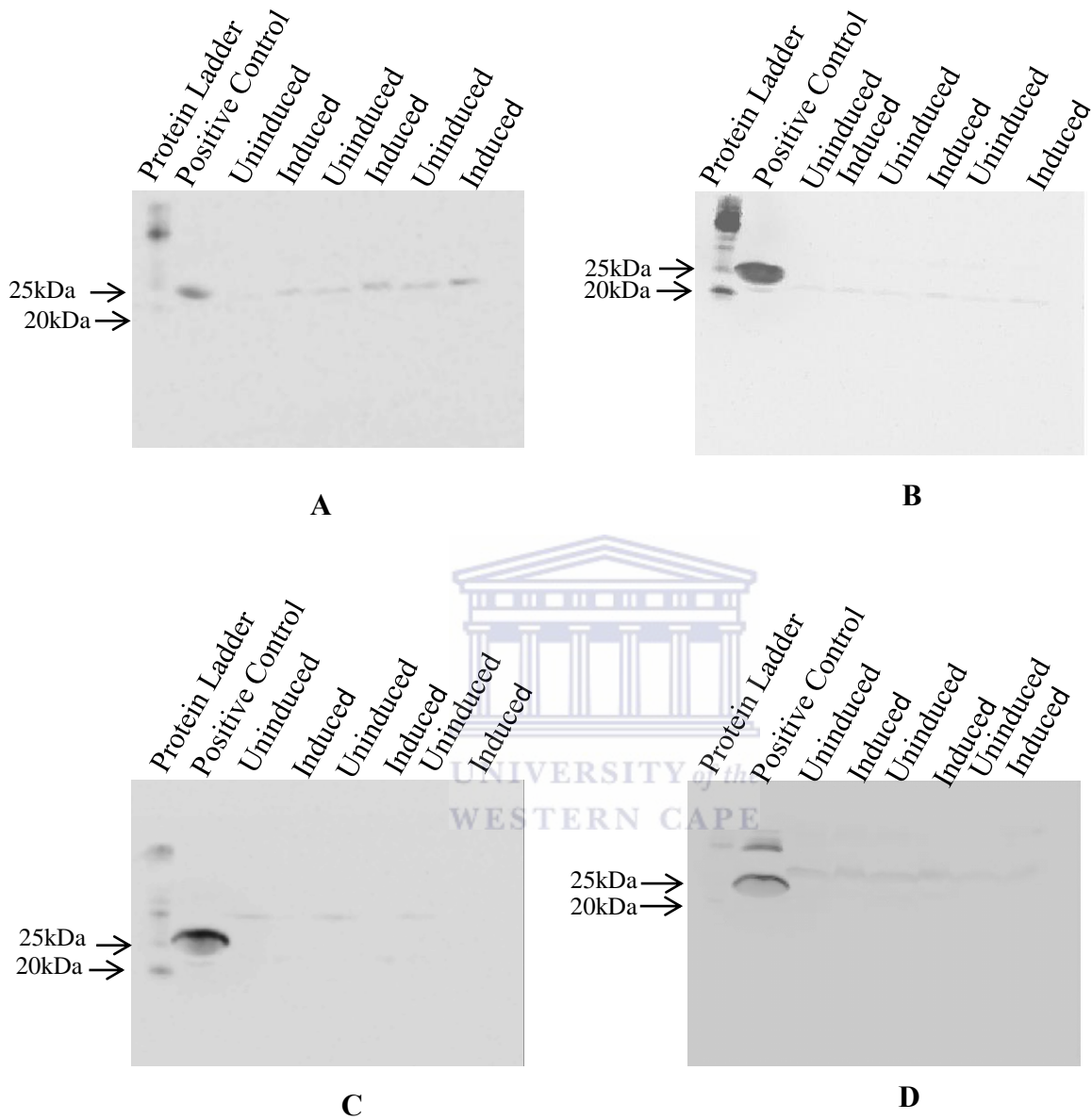


Figure 3.6: Western blot analysis of bacterial lysates. A shows p6.1, B shows p.L, C shows MV and D shows NL1.1. Peptide expression was induced using 1mM IPTG. Peptides were expressed in BL21 *E.coli* cells.

3.2.3. Screening for the presence of peptides in culture medium

Screening of the peptides in bacterial lysates using expression screen by coomassie and western blot analysis did not confirm the presence of the peptides. Literature has shown that expressed peptides are sometimes secreted into the culture medium (Uhlen and Abrahmsen, 1989). Therefore to investigate whether the bacterial cells secreted the peptides into the culture medium, protein expression was induced by IPTG and the culture medium was screened for the presence of the peptides. The cells were separated from the culture medium and all the proteins present in the medium were precipitated as described in section 2.8.1. The samples were analyzed by SDS PAGE. Major bands with a molecular weight of less than 10kDa were present in both uninduced and induced precipitates as shown in Figures 3.7.

To investigate whether these low molecular weight proteins were likely to be the peptides of interest, a western blot analysis was performed on the precipitated protein samples using the anti-histidine antibody as described in section 2.10.2 (Figure 3.8). InlC, a 25kDa protein was detected for the positive control. However histidine tagged peptides could not be detected in the precipitated protein samples generated from the medium in which the bacteria was cultured.

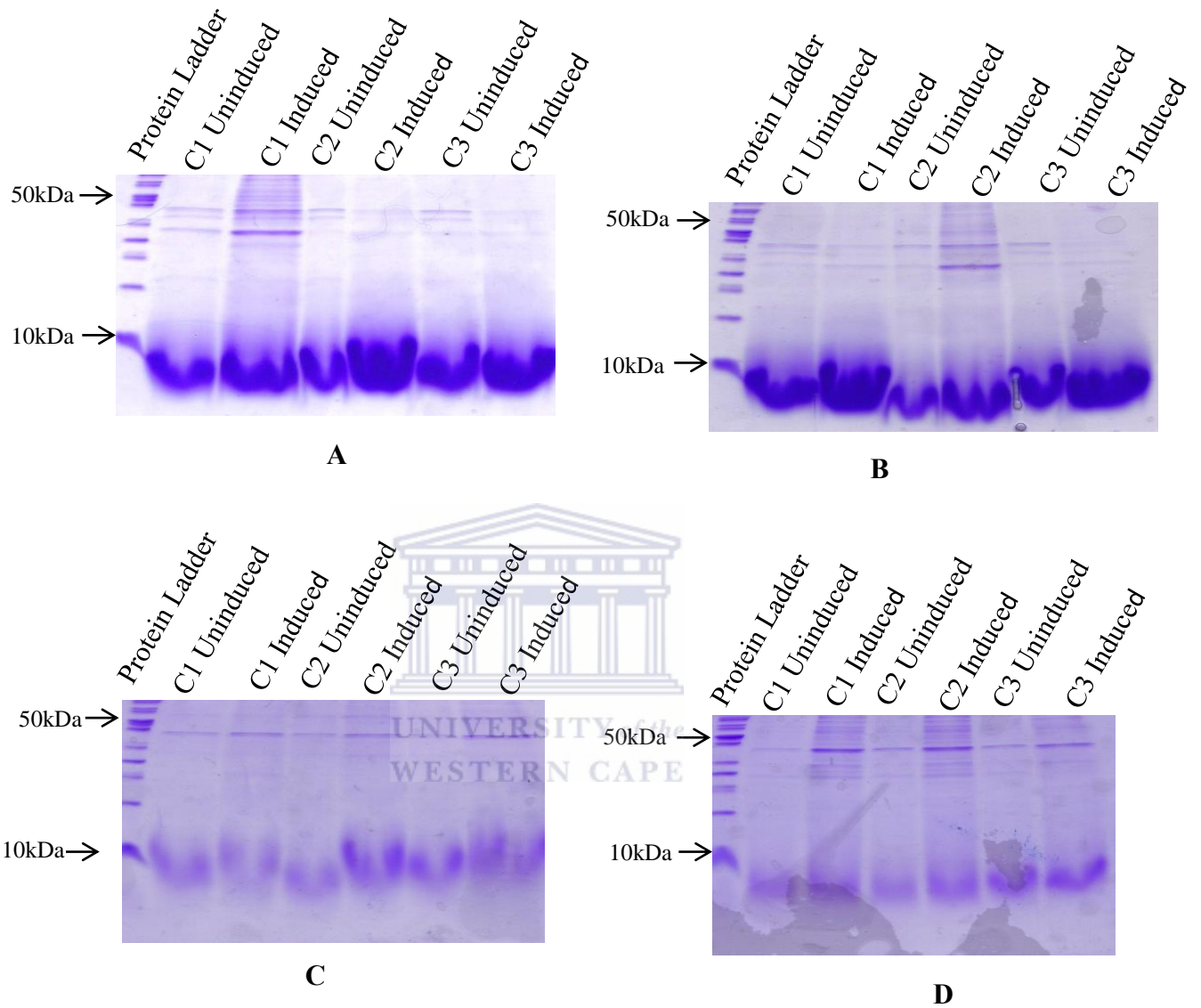


Figure 3.7: SDS PAGE analysis of precipitated protein secreted in culture medium. *E. coli* cells were transformed with pET21b peptide containing sequences encoding the peptides. A shows expression screen of p6.1 in BL21 (DE3), B shows screening of p.L BL21 (DE3), C shows screening of MV in arctic express and D shows screening of NL1.1 in BL21 codon plus. Three colonies were selected for each peptide (C1-C3). The bacteria was induced using 1mM IPTG. The expression profile was resolved on an 18% SDS polyacrylamide gel.

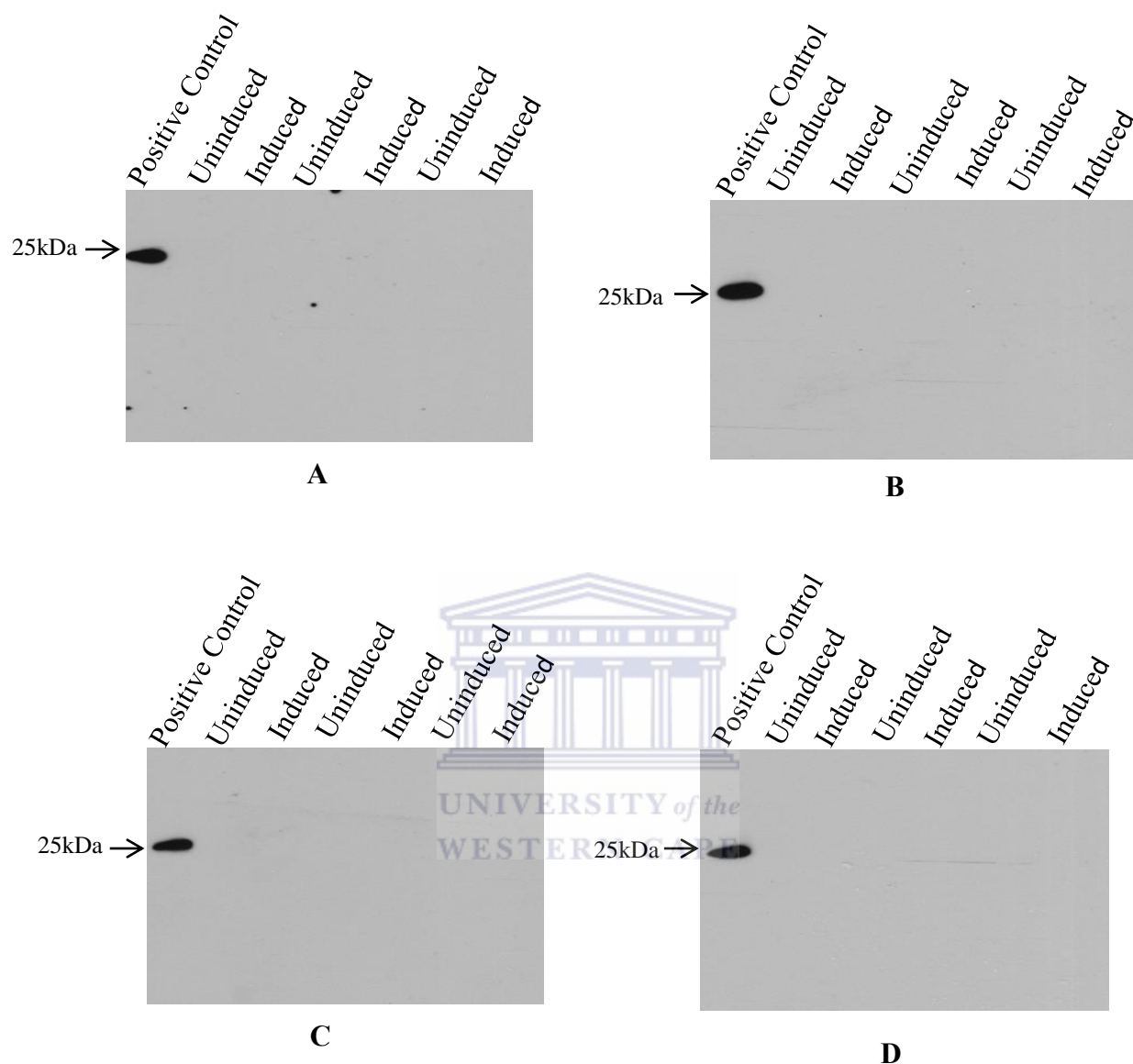


Figure 3.8: Western blot analysis of precipitated protein secreted in culture medium. A shows p6.1 in BL21(DE3), B shows p.L expressed in BL21(DE3), C shows MV peptide expressed in arctic express and D shows NL1.1 peptide expressed in BL21 codon plus. Protein expression was induced using 1mM IPTG. The expression profile was resolved on an 18% SDS polyacrylamide gel.

3.4. Discussion

The aim of this chapter was to recombinantly express cancer targeting peptides. The oligonucleotides encoding the peptides p6.1, P.L, NL1.1 and MV were successfully cloned into pET21b plasmid vector. Sequence analysis of the clones showed the correct translated protein sequence of the peptides. There were no mutations present and sequences displayed the histidine tag (Figure 3.1 A-D).

Following successful cloning of the oligonucleotides, the next phase was to express the peptides using an expression host. Expression was carried out using *E.coli* BL21 (DE3). The bacterial lysates were examined by coomassie using SDS polyacrylamide gels. The calculated peptide sizes were 1.78kDa for p6.1, 1.97kDa for p.L, 2.52kDa for MV and 3.3kDa for NL1.1. Inspection of the gels did not show any low molecular weight bands of sizes below the 10kDa molecular weight marker (Figure 3.5 A-D). This could have been due to low expression of the peptides such that analysis by coomassie was not adequate to detect the peptides. Therefore western blot analysis which is more sensitive than coomassie was utilized to detect the low molecular weight peptides

The oligonucleotides were cloned so as to include a histidine fusion tag. Sequence analysis of the clones showed that the sequences were histidine tagged (Figure 3.4 A-D). Hence the anti-histidine antibody was used in the western blot analysis to detect the histidine tag and hence the peptides. A protein of 25kDa (InlC) containing a histidine tag was included and served as a positive control. This protein was clearly detected by western blot analysis as shown in Figures 3.6 A-D. However low molecular weight bands of sizes 1.78kDa-3.33kDa were not detected by western blot. Hence it was concluded that the peptides were not present in the bacterial lysate. The Figures in 3.6 also

show high molecular weight bands in the induced and uninduced samples. These bands are possibly as a result of spill over from the positive control.

Literature has shown that proteins expressed recombinantly are sometimes secreted into the culture medium (Uhlen and Abrahmsen, 1989). To investigate if the expressed peptides were secreted into culture medium, proteins in culture medium were precipitated and analysed by coomassie. Analysis by coomassie showed major bands that were less than 10kDa as indicated by the molecular weight marker (Figure 3.7 A-D). To investigate if these bands were the expressed peptides, western blot analysis using the anti-histidine tag was carried out. The analysis showed a 25kDa histidine tagged protein, but failed to detect the low molecular weight peptides in the induced and uninduced culture medium samples. Although the oligonucleotides encoding the peptides were successfully cloned, it was concluded that peptide expression was not successful.

A number of reasons can be elucidated as to why peptide expression in *E. coli* using pET21b vector was not efficacious. One plausible reason can be attributed to ATP dependent proteolytic enzymes that are found inherently in the host cells. Proteolytic enzymes function to maintain cell metabolism and cell growth for the host cell among other functions (Gottesman *et al.*, 1997). Proteolytic enzymes act by cleavage of amide bonds resulting in individual amino acids. At times proteolytic action by the proteases is complete such that no intermediate products are detectable.

In comparison to other peptides that have been expressed recombinantly as shown by literature (Satakarni and Curtis, 2011; Metlitskaia *et al.*, 2004; Bosse-Doenecke *et al.*, 2008), the cancer targeting peptides that were to be expressed are relatively small. For example Satakarni and Curtis were able to synthesize a peptide of 11.5kDa. In comparison the largest cancer targeting peptide that was to be expressed in our study was 3.3kDa. Hence owing to the fact the peptides were

significantly small and probably linear, it is hypothesized that the peptides were easily accessible to the proteolytic enzymes and hence susceptible to degradation.

3.5. Limitations and recommendations

Limitations in expression of cancer targeting peptides included use of a limited number of bacterial hosts some of which could have housed proteolytic enzymes. The main expression host used was BL21 (DE3) and it is naturally deficient in the lon protease and does not have the ompT outer membrane protease that can degrade proteins. However the host could have housed other proteases and peptidases that could have caused proteolytic degradation. (Novagen, 2003). If unsuccessful expression of the peptides was due to proteolytic cleavage of the peptides, then use of hosts without proteolytic enzymes would have resulted in successful expression of the peptides. Kandilogiannaki and others used hosts without proteolytic enzymes which resulted in successful expression of an anti-MUC1 scFv fragment (Kandilogiannaki *et al.*, 2001).

An avenue that was approached to achieve peptide expression to avoid proteolytic enzymes was *in vitro* expression or cell free expression. The principle of cell free expression system lies in the mimicry of protein expression that occurs in intact cells. As the name suggests a cell free expression system synthesizes protein outside the cell by using either DNA or exogenous RNA as a template (Jackson *et al.*, 2003). A requirement of the template is that it should contain the necessary regulatory elements. The machinery of the cell free system constitute crude cell extract as well as external supply of amino acids energy sources in form of adenosine triphosphates (ATP), salts, nucleotides and amino acids. The most commonly used cell free expression systems are those derived from *E.coli* (Jackson *et al.*, 2003). The cell free expression did not yield detectable

expressed peptides and hence this avenue needs optimization and will be approached again in the future.



CHAPTER 4

4.1. Conjugation of cancer specific peptides to quantum dots

4.1.1. Introduction

Since attempts to express the peptides in bacteria were unsuccessful, the peptides were obtained commercially. The peptides p6.1, p.L, NL1.1 and MV were purchased from GL biochem (Shanghai) in a lyophilized form to ensure stability. The p6.1 and p.L peptides were successfully dissolved while the NL1.1 and MV peptides did not dissolve in the recommended solvents. Hence due to insolubility, these two peptides were not used in further experiments. The panel of peptides was expanded and included p.C, Frop-1 and p.H which were identified from literature (Shadidi and Sioud, 2003) and these were purchased from GL biochem (Shanghai). The final list of peptides used in the experiments is shown in Table 2.11. EDC chemistry was used to conjugate the peptides to carboxyl functionalized quantum dots through amide bond formation as described in Section 2.13. The aim was to study the binding of the peptides to cancer cells. The conjugation of peptides to quantum dots (QD 525) made it possible to investigate the binding of the peptides using techniques such as flow cytometry and fluorescence microscopy.

Amide bonds occur in a variety of biological molecules and are constituents of various synthetic molecules. As such amide bonds play important roles in biological processes such as catalysis by means of enzymes, control of cell growth and cell differentiation as well as immune responses by means of antibodies (Martinez *et al.*, 2003). Organic chemistry and pharmaceutical chemistry use various synthetic molecules that are the basis for formulation of products such as drugs and

peptides all which are dependent on successful amide bond formation (Pattabiraman and Bode, 2011).

The formation of an amide bond occurs between a carboxylic acid and an amine through a condensation reaction. In non-biological systems, formation of the amide bond is not a spontaneous process so much so that it does not occur at all at room or ambient temperatures. On the contrary, reactions between carboxyl groups and amino groups at ambient temperatures result in the formation of a carboxylate ion instead of the desired amide bond. Amide bond formation requires a high input of energy in the form of high temperatures, which in the case of peptide formation would be detrimental to the product (Valeur and Bradley, 2009). Therefore fields such as organic and medicinal chemistry employ the use of coupling reagents to coadunate the carboxyl and amino groups resulting in amide bonds.

Amongst the most commonly used coupling reagents are carbodiimides such as EDC. This zero length cross linker molecule forms amide bonds by first activating the carboxylic acid group to form an active o-acylisourea intermediate. This highly reactive intermediate then reacts with the amino group forming an amide bond (Nakajima and Ikada, 1994). This method of amide bond formation is also called EDC chemistry and it was used in this study to conjugate synthetic peptides to quantum dots carrying a carboxyl functional group.

4.1.2. Quantification of the binding of peptide-quantum dot conjugates to cells using flow cytometry and fluorescence microscopy

A panel of human cell lines, which included Caco-2, Hela, HepG2, HT29 and Kmst-6 were used to do a comparative study on the peptides evaluating the ability of the peptides to bind to the cells. Since the peptides were conjugated to quantum dots, the quantification of the fluorescence

intensity was used to assess the ability of the peptide-quantum dot conjugates to bind to the cells. The geometric median fluorescence intensity was used as a measure of fluorescence intensity. Figure 4.1. shows the binding of the different peptide quantum dot conjugates to the cancer cell lines as well as Kmst-6. Figures 4.2-4.6 shows fluorescence microscopy images and the corresponding fluorescence intensity graphs by flow cytometry.



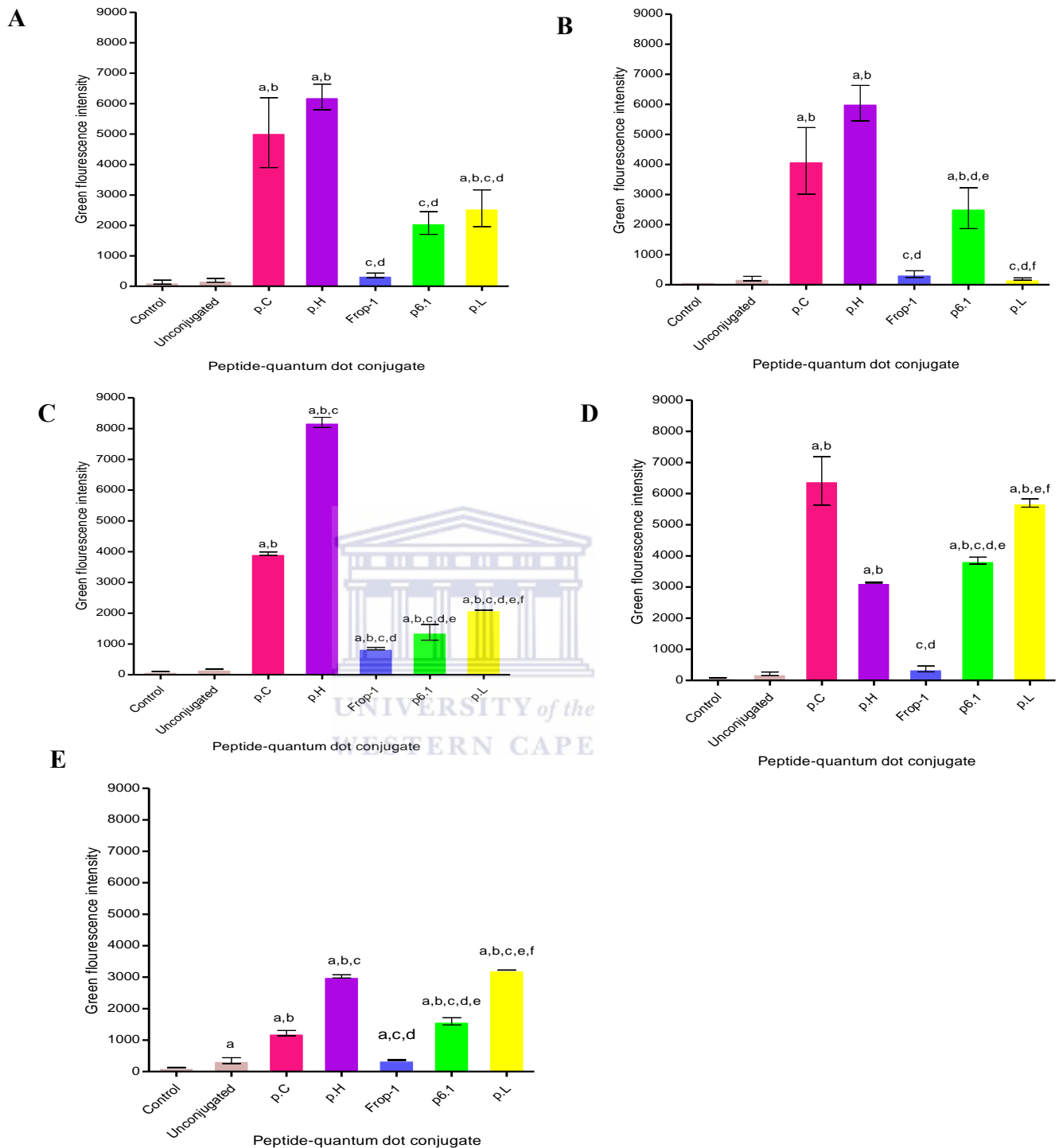


Figure 4.1: Targeted binding of peptide conjugated quantum dots 525 to cancer cells. **A** shows binding of the different peptide-quantum dot conjugates to Caco-2 cells. **B** shows binding of the conjugates to HeLa cells. **C** shows binding of the conjugates to HepG2 cells, **D** shows binding of the conjugates to HT29 and **E** shows binding of the conjugates to Kmst-6 cells. The bar graphs from left to right are understood as labelled **a**, **b**, **c**, **d** and so on. The superscripts denoted on the bar graphs indicate the statistical significance in binding between the conjugates. For example superscript **a** denoted on bar graph **b** shows that there is a significant difference in binding between **a** and **b** ($P < 0.05$).

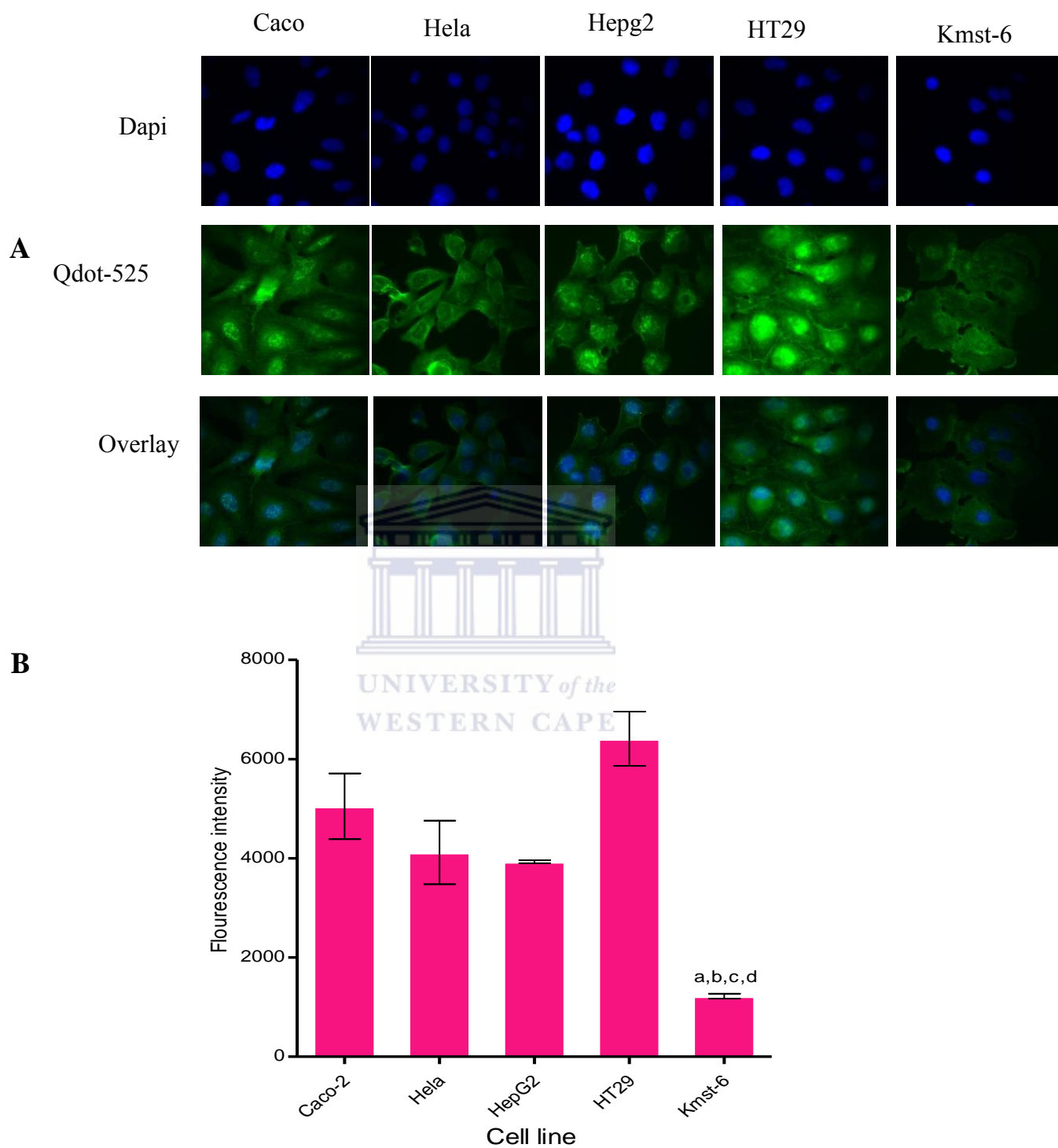


Figure 4.2: Binding of p.C-Qdot 525 conjugate to cancer cells. **A** shows microscopy analysis of cancer cells stained with the peptide-quantum dot complex. **B** shows flow cytometry analysis of the cancer cell lines. Standard deviations are also shown ($P < 0.05$).

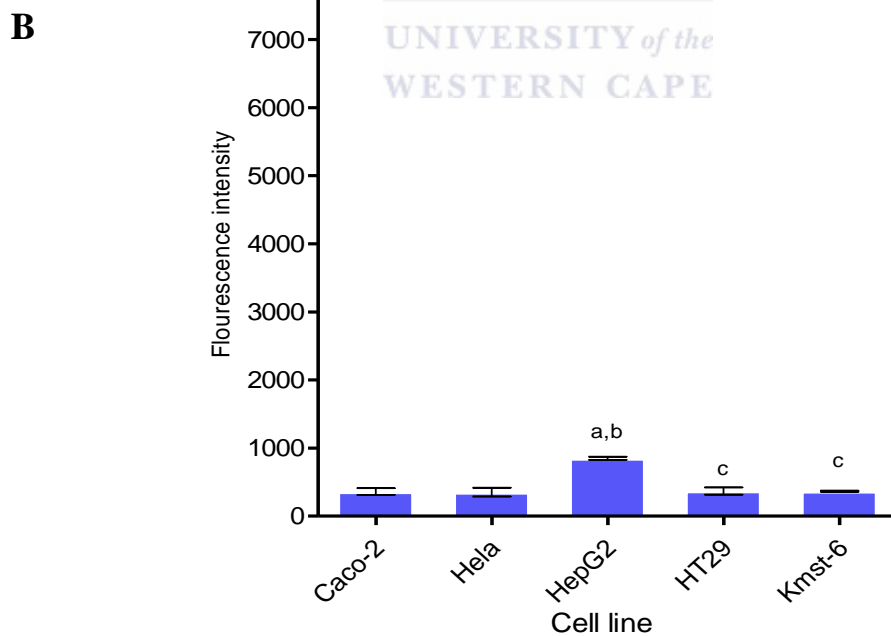
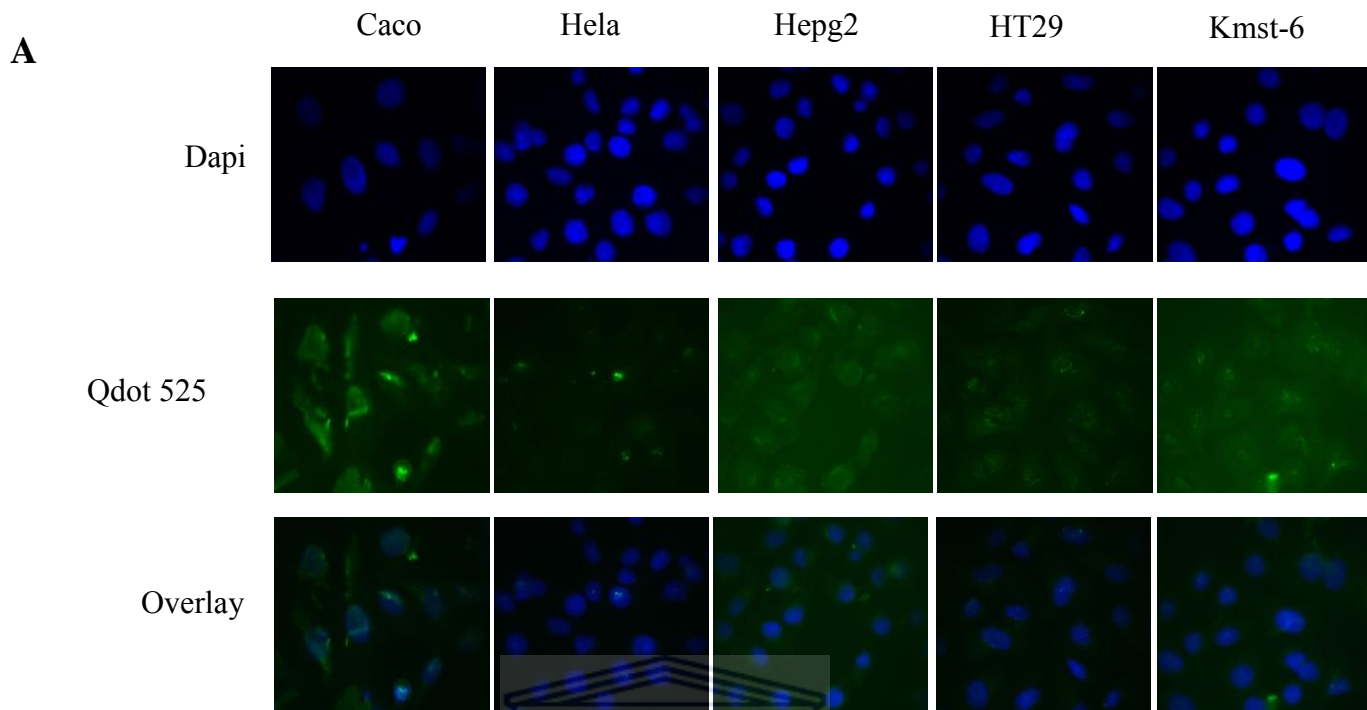


Figure 4.3: Binding of Frop-1-Qdot 525 conjugate to cancer cells. **A** shows microscopy analysis of cancer cells stained with the peptide-quantum dot complex. **B** shows flow cytometry analysis of the cancer cell lines. Standard deviations are also shown ($P < 0.05$).

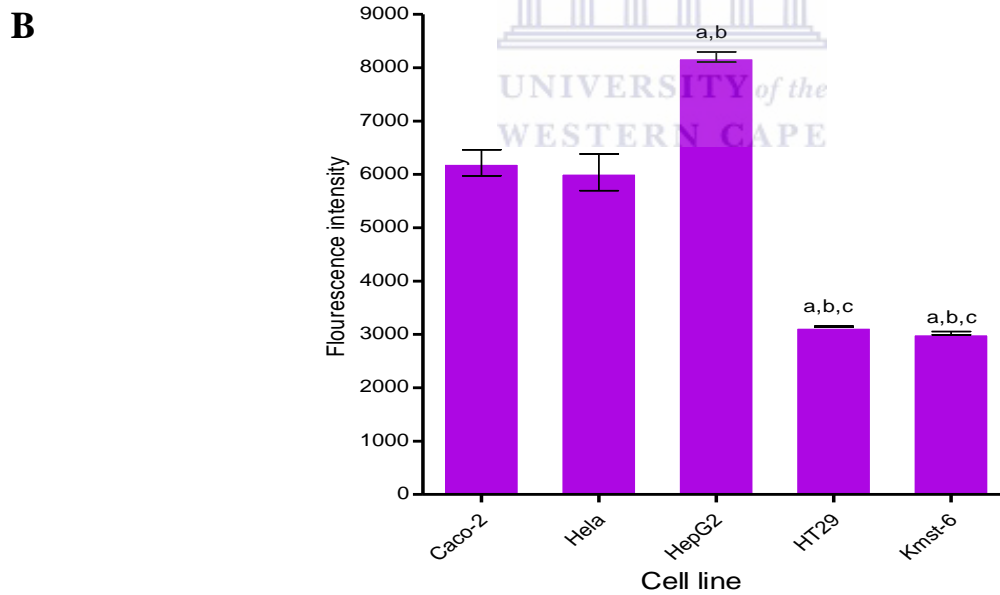
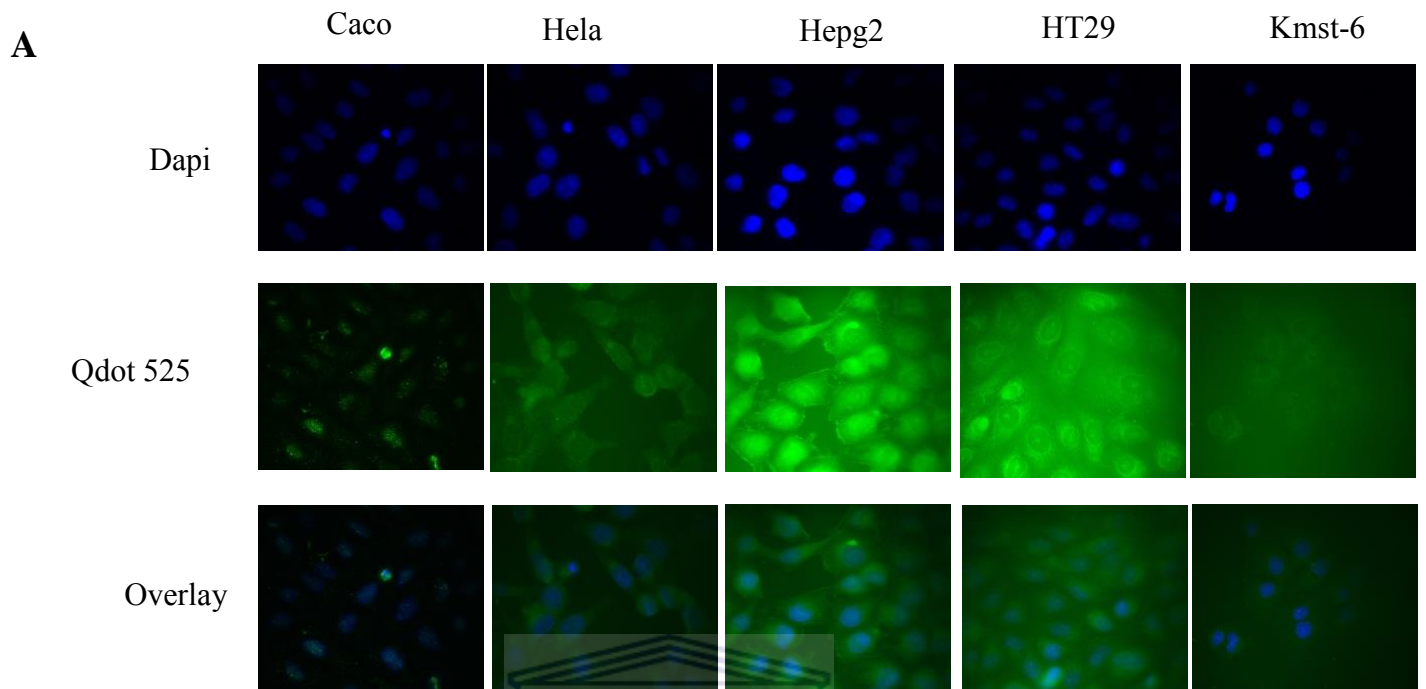
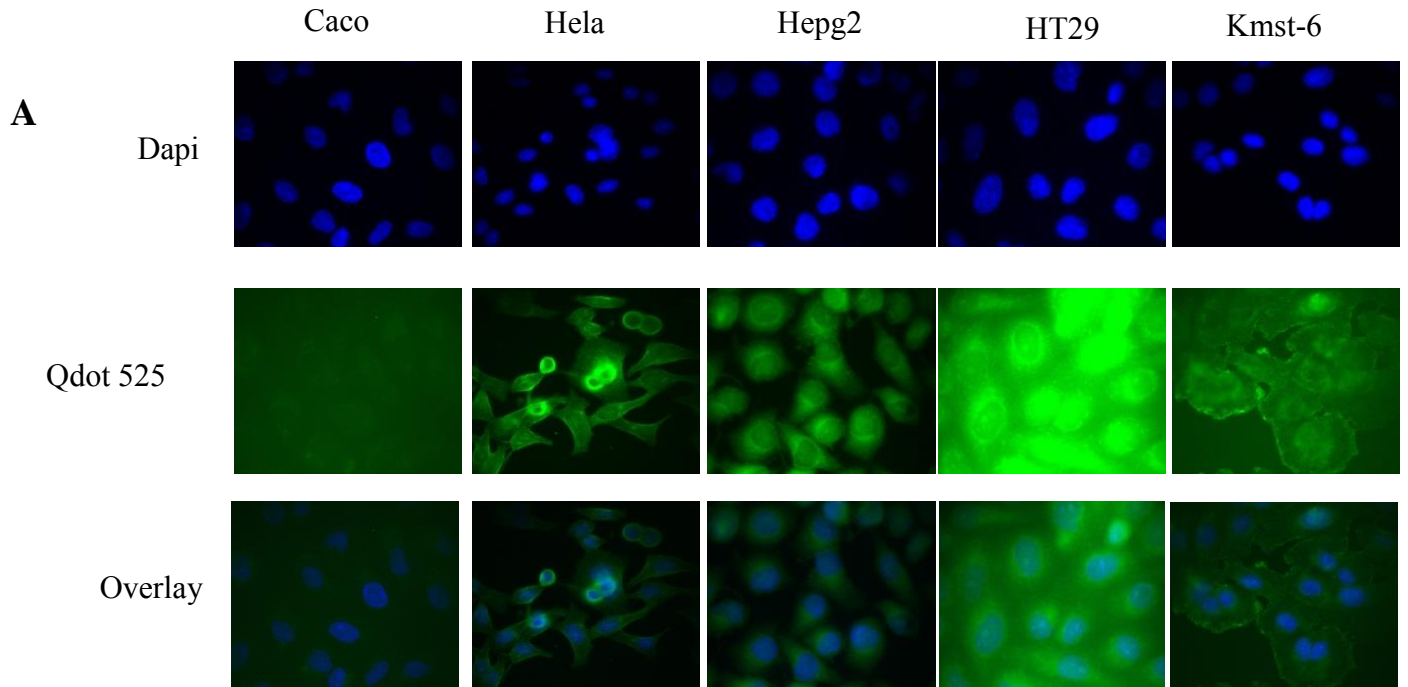


Figure 4.4: Binding of p.H-Qdot 525 conjugate to cancer cells. **A** shows microscopy analysis of cancer cells stained with the peptide-quantum dot complex. **B** shows flow cytometry analysis of the cancer cell lines. Standard deviations are also shown ($P < 0.05$).



B

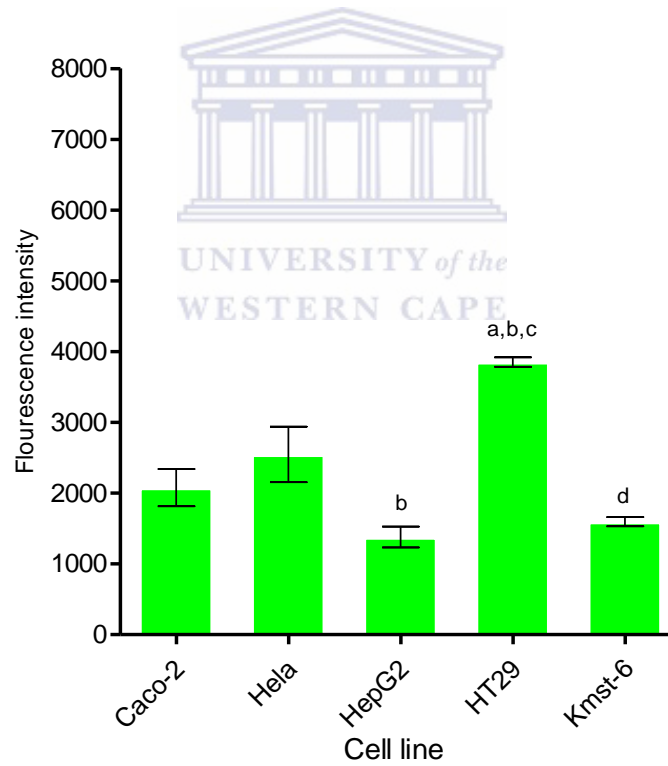


Figure 4.5: Binding of p6.1-Qdot 525 conjugate to cancer cells. **A** shows microscopy analysis of cancer cells stained with the peptide-quantum dot complex. **B** shows flow cytometry analysis of the cancer cell lines. Standard deviations are also shown ($P < 0.05$).

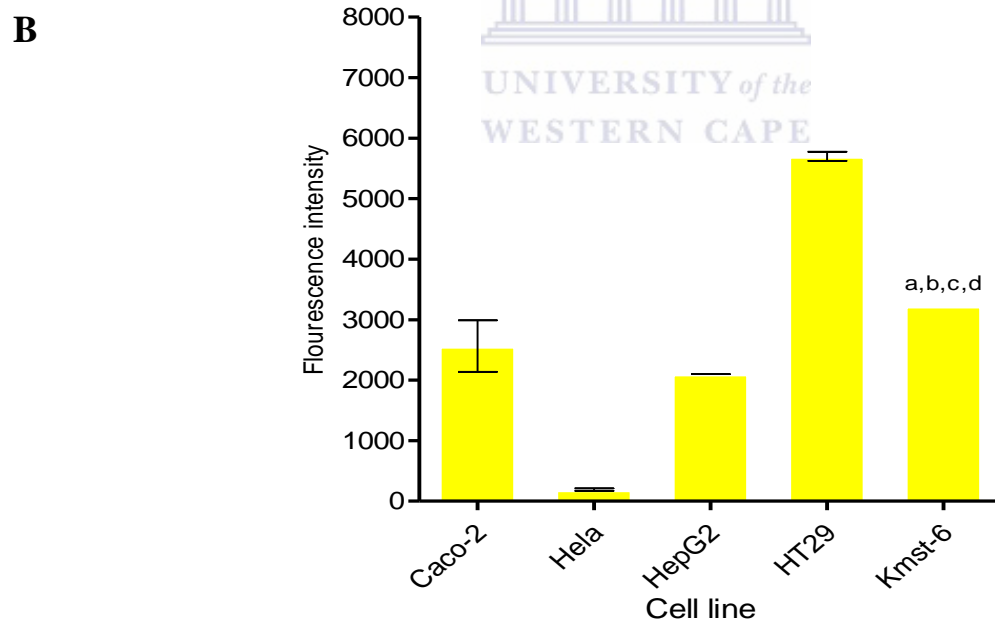
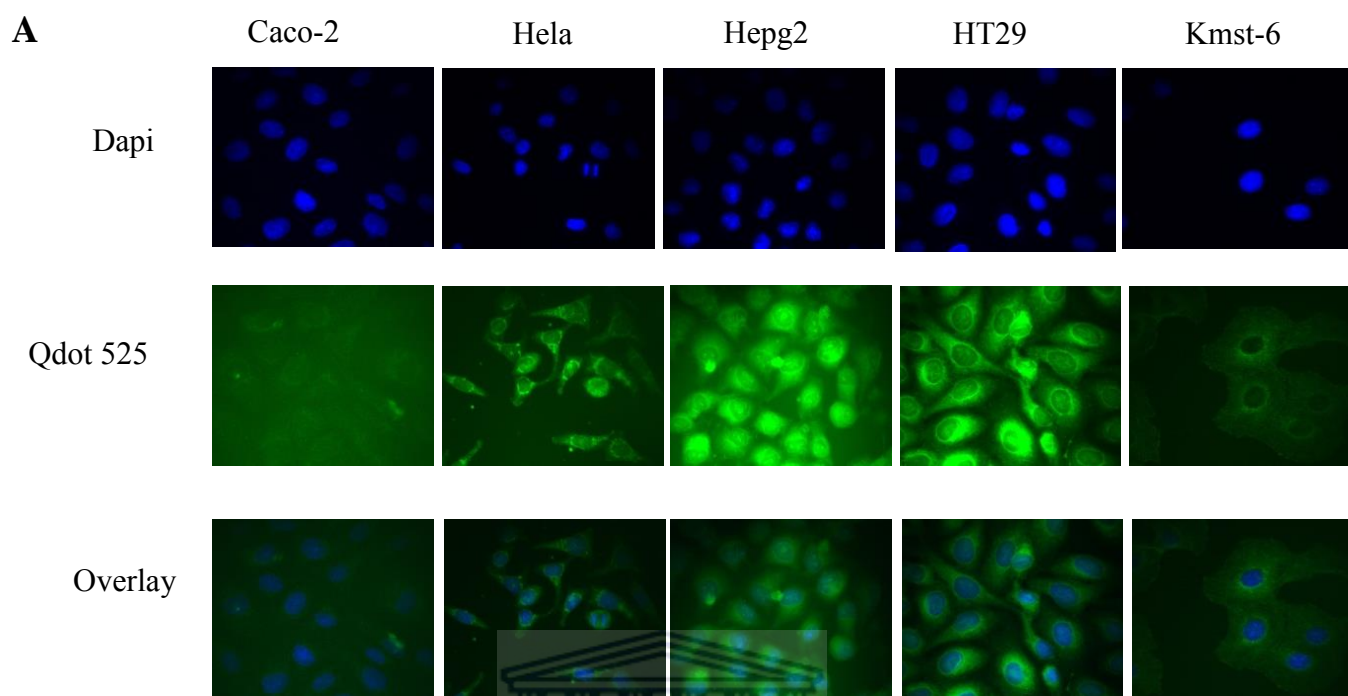


Figure 4.6: Binding of p.L-Qdot 525 conjugate to cancer cells. **A** shows microscopy analysis of cancer cells stained with the peptide-quantum dot complex. **B** shows flow cytometry analysis of the cancer cell lines. Standard deviations are also shown ($P < 0.05$).

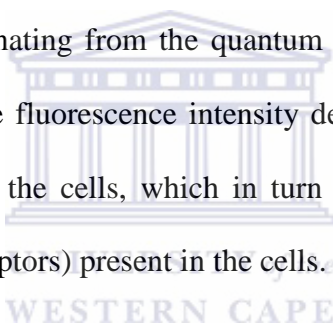
4.2. Summary

The peptides namely p.C, p.H, Frop-1, p6.1 and p.L were conjugated to carboxyl quantum dot 525. The peptide-quantum dot conjugates were then targeted to different cancer cells lines. Fluorescence microscopy and flow cytometry were used to assess binding of the cancer targeting peptides.



4.3. Discussion

The main aim of the study was to investigate the binding of cancer specific peptides to a panel of human cancer cells and thus determine the specificity of the binding of these peptides. The study was conducted on 4 human cancer cell lines (Caco-2, Hela, HepG2 and HT29) and 1 non-cancerous (Kmst-6) human cell line. Indication from the literature is that these peptides bind specifically to receptors expressed in cancer cells. These receptors are either absent from non-cancerous cells or they are expressed at low levels in non-cancerous cells. The peptides were conjugated to quantum dots and the cells were exposed to the peptide-quantum dot conjugates. The cells were analyzed by flow cytometry and fluorescence microscopy and by measuring the intensity of the fluorescence originating from the quantum dots, the binding specificity of the peptides could be determined. The fluorescence intensity depended on the number of peptide-quantum dot conjugates bound to the cells, which in turn depended on the number of target biomolecules (e.g. cell surface receptors) present in the cells.



Five peptides (p.C, p.H, Frop-1, p.6.1 and p.L) were investigated in this study. The fluorescence intensities obtained when the quantum dots were conjugated with the peptides were significantly higher than the fluorescence intensities obtained for the unconjugated quantum dot controls. This suggests that the peptides were able to specifically bind to the cells. This was true for all the peptides in all the cell lines tested in this study, except for Frop-1. No significant difference could be observed between Frop-1 conjugated quantum dots and unconjugated quantum dots in Caco-2, Hela, HT29 and Kmst-6 cells. HepG2 is the only cell line where significant difference could be observed between Frop-1 conjugated quantum dots and unconjugated quantum dots. This suggests that the peptides were able to differentiate between the different cell types. Although a significant variation in the intensity of the fluorescence was observed for the different peptides and the

different cell lines, it must be noted that the fluorescence intensities obtained for quantum dots conjugated with Frop-1 was much lower than the fluorescence intensities obtained for the other peptides. The selectivity of the peptides was also very well demonstrated with the p.L peptide. This peptide was able to bind to Caco-2, HepG2, HT29 and Kmst-6 cells, but not Hela cells. It is also evident that the fluorescence intensities obtained for the non-cancerous cell line, Kmst-6 was generally lower than the fluorescence intensities obtained for the cancerous cell lines, Caco-2, HepG2, HT29 and Hela. This is in line with the expectation that the expression levels of the targets for these peptides should be lower in non-cancerous cells compared to cancer cells.

The binding of the peptide-quantum dot conjugates to the cells was also studied by fluorescence microscopy. Fluorescence microscopy showed a variation in fluorescence intensity and there was a very good correlation between the quantitative analysis obtained by flow cytometry and the microscopy results. There was also an indication that the localization of the peptide-quantum dot conjugate staining was not the same for all the cell lines. As an example, quantum dots conjugated with the p.L peptide appear to be localized in the cytoplasm of HT29 cells, with minimal staining in the nucleus (Figure 4.6 A). However, in HepG2 cells the peptide-quantum dot conjugates appear to be distributed evenly throughout the cells. This observation is more evident in the overlaid images of DAPI and Qdot525. This may point to either different targets being present in the different cell types or the same target being present in different locations in the cells. However, higher resolution microscopy is required to confirm these findings.

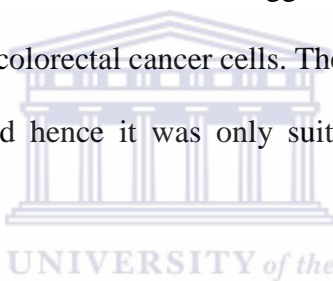
The results for p.C-Qdot-525 conjugate (Figure 4.2 A) showed strong binding specificity of the peptide to the all cancer cell lines. Differential binding specificity was observed between the non-cancerous Kmst-6 cell line and the cancer cell lines (Figure 4.2 B), since the fluorescence intensity was significantly different between Kmst-6 cells and the cancer cells. This finding suggested that the p.C peptide does not bind to the non-cancerous cells with high specificity and can possibly be used to differentiate between cancerous and non-cancerous cells. However, a larger panel of both cancerous and non-cancerous cell lines should be investigated. The p.C peptide was discovered using a random phage display library and was raised against prostate specific antigen. According to the study carried out by Wu and others this peptide showed binding specificity towards prostate cancer cells (Wu *et al.*, 2000). However, none of the cancer cell lines used in this study is of prostate cancer origin.

The microscopy results confirmed the low binding efficiency of the Frop-1-Qdot-525 conjugate to all the cell lines used in this study. The average fluorescence intensity for this peptide was less than 1000 FI units, which is very low when compared to the other peptides used in this study (Figure 4.3B). Even though the binding efficiency of this peptide was very low, there was still a significant difference in binding of the Frop-1-Qdot-525 conjugate to HepG-2 cells. This showed that the Frop-1 peptide bound with a greater specificity to the HepG-2 cells. These findings possibly suggested that conjugation between the peptide and the quantum dot did not take place or that the peptide does not bind to the cancer cells.

It was previously reported that the Frop-1 peptide is highly unstable. The authors reported that the Frop-1 peptide stability was improved by attaching it to 1, 4, 7, 10-tetraazacyclododecane-1, 4, 7, 10-tetraacetic acid (DOTA). The attachment of DOTA improved the stability of the peptide in serum to 71 minutes, while the Frop-1 peptide without the chelator was only stable in serum for

15 minutes (Mier *et al.*, 2013). It is therefore possible that the attachment of DOTA can significantly increase the targeting specificity of Frop-1.

The highest fluorescence intensity (~8000 FI units) was obtained for the p.H peptide in HepG2 cells (Figure 4.4). Based on the fluorescence intensity, this peptide was not able to discriminate between Caco-2 and Hela cells or HT29 and Kmst-6 cells. Discovered by random phage display library, the p.H peptide was raised against human colorectal cancer cells (WiDr). Binding to MDA-MB-435 breast cancer cells was demonstrated by Rasmussen and others for this peptide. The authors demonstrated that the peptide also had high binding affinity to Hela cells. This was confirmed in the current study. The authors therefore suggested that the receptors targeted by the p.H peptide were not unique to the colorectal cancer cells. They also reported that the cancer cells did not internalize the peptide and hence it was only suitable for application in diagnostics (Rasmussen *et al.*, 2002).



The highest fluorescence intensity for the p6.1 peptide was in HT29 cells (Figure 4.5). Compared to p.C and p.H, the p6.1 peptide did not bind the cancer cells with high affinity. The fluorescence intensity for p6.1 was only about ~3800 FI units for HT29. This peptide was previously shown to bind to cancer cells that overexpress the ErbB2 receptor as well as prostate and breast carcinoma (Karasseva *et al.*, 2002).

The highest fluorescence intensity for the p.L peptide was in HT29 cells (Figure 4.6) with fluorescence intensity of ~6000 FI units and this was confirmed by microscopy. p.L peptide had the least binding affinity to Hela cells with FI units of only ~1000. Wang and others reported that the p.L peptide has a higher binding specificity toward cancer cells that over express the ErbB-2 growth factor receptor (Wang *et al.*, 2008). Microscopy images of the cells stained with p.L-Qdot-

525 conjugate shown in Figure 4.6 A, showed that the peptide showed a similar binding pattern of cells as did the flow cytometry analysis. Microscopy analysis showed strong binding of the p.L peptide to HeLa, HepG-2 and HT29 cells. Elucidation of P-values indicated that the Kmst-6 cell line showed the lowest binding with a significant difference in binding in comparison to the cancer cell lines. This result once again showed that the cancer targeting peptides bound with high efficiency to cancer cells and not the normal cell line. As shown by Shadidi and Sioud as well as Haglund and others, this peptide binds also to breast cancer cells. The peptide also has the ability to cross the cell membrane as it was shown to successfully deliver anti-sense oligonucleotides to breast cancer cells for the purpose of down regulating ErbB2 expression (Shadidi and Sioud, 2003). Hence the LTV peptide can be used for cancer diagnostic as well as therapeutics.

The binding of the cancer targeting peptides (used in this study) to cancer cells has only been demonstrated in some selected cancer cell lines. The binding of the p.C peptide has only been investigated in a prostate cancer cell line (Wu *et al.*, 2000), while the binding of the p.L peptide has only been investigated in breast cancer cells (Haglund *et al.*, 2008; Shadidi and Sioud, 2003). As such these peptides have not been very well characterized. This study provided a platform to characterize the binding of these peptides to different types of cancer cells by using a panel of human cell lines. Characterization of these peptides in this manner is important as these peptides can be strategically used in cancer diagnosis as well as to specifically direct cytotoxic agents to cancer cells *in vivo*.

The study also demonstrated the superlative optical properties of quantum dots. Continual fluorescence from the peptide conjugated quantum dots was observed following prolonged illumination from a light source during microscopy analysis. This property of quantum dots is advantageous in comparison to organic fluorophores, which are subject to photobleaching as

indicated in literature (Zhou and Ghosh, 2006). This study shows that some of the cancer targeting peptides investigated here together with quantum dots have a real potential for application in cancer diagnosis and therapeutics. For example peptides conjugated to quantum dots that emit in near infrared wavelengths can be used *in vivo* to detect and hence diagnose cancer. Additionally, the peptide quantum dot conjugates can be used as vehicles to deliver anti-cancer agents *in vivo* and hence specifically target and treat cancer cells without harming the healthy cells. This avenue in therapeutics is attractive as the adverse effects caused by cytotoxic agents can be greatly minimized.

4.3.1. Conclusion

This study demonstrated that the cancer targeting peptides used in this study bind to cancer cells and that the specificity with which these peptides bind to the cells depends on the cell types and the peptide. Based on the fluorescence intensity at least one of the peptides, namely p.C was able to differentiate between the cancer cell lines and the non-cancerous cell line. This peptide can possibly be used for the targeted delivery of drugs to cancer cells or applied in the diagnosis of cancer. The binding specificity of the p.H peptide was shown to be the highest amongst all the peptides tested in this study.

4.4. Future Directions

4.4.1. Limitations of the study

Cancer cell targeting using the Frop-1 peptide showed very low levels of binding affinity to the cancer cell lines. The binding in some instances was comparable to cells that were stained with unconjugated Qdot-525 and to cells that were not stained. Instability of the Frop-1 peptide could have contributed to the low levels of binding. Stability of the Frop-1 peptide has been shown to have been improved by attaching the peptide to a chelator, DOTA. Studies have shown that the Frop-1 peptide has been successfully targeted to thyroid (Fro82-2), MCF-7, cervix, prostate carcinoma and cell lines from head and neck tumors. Hence the binding specificity of the Frop-1 peptide with DOTA needs to be evaluated. It is also possible that the Frop-1 peptide was not successfully conjugated to the quantum dots hence conjugation of the peptides to the quantum dot need to be evaluated using quantitative methods. Another limitation is that only four cancer cell lines were assessed. More cancer cell lines need to be assessed for their response to cancer targeting peptides. This will give precise indication as to which cancer targeting peptides bind with specificity in particular cancer cells. This in turn will give more direction as to how these cancer targeting peptides can be applied in cancer diagnosis.

References

- Aina, O., Liu, R., Sutcliffe, J., Marik, J., Pan, C. and Lam, K. (2007) From combinatorial chemistry to cancer-targeting peptides. *Molecular Pharmaceutics*, **5**: 631–651.
- Alivisatos, A., Gu, W. and Larabell, C. (2005) Quantum dots as cellular probes. *Annual Review Biomedical Engineering*, **7**: 55-76.
- Andeson, M.H., Becker, J. and Straten, P.T. (2005) Regulators of apoptosis: suitable targets for immune therapy of cancer. *Nature Review Drug Discovery*, **4**: 399-409.
- Anderson, M.W., Reynolds, S.H., You, M. and Maronpot, R.M. (1992) Role of proto-oncogene activation in carcinogenesis. *Environmental Health Perspectives*, **98**: 13-24.
- Andrae, J., Gallini, R. and Betsholtz, C. (2008) Role of platelet-derived growth factors in physiology and medicine. *Genes and development*, **22**: 1276-1312.
- Arteaga, C.L. (2002) Epidermal growth factor receptor dependence in human tumors: more than just expression? *The Oncologist Supplement*, **4**: 31-39.
- Askenazi, A. and Dixit, V.M. (1999) Apoptosis control by death and decoy receptors. *Current Opinion in Cell Biology*, **11**: 255-260.
- Azzazy, H.M.E., Mansour, M.H.M. and Kazmierczak, S.C. (2007) From diagnosis to therapy: Prospects of quantum dots. *Clinical Biochemistry*, **40**: 917-927.
- Bai, L. and Zhu, W. (2006) p53: Structure, function and therapeutic applications. *Journal of Cancer Molecules*, **4**: 141-153.

Bargmann, C. I., Hung, M. C. and Weinberg, R. A. (1986) The Nue oncogene encodes an epidermal growth factor receptor protein. *Nature*, **319**: 226-230.

Baylin, S.B., Esteller, M. and Rountree, M.R. (2001) Aberrant patterns of DNA methylation, chromatin formation and gene expression in cancer. *Human Molecular Genetics*, **10**: 687-92.

Bearss, D.J., Hurley, L.H. and Von Hoff, D.D. (2000) Telomere maintenance mechanisms as a target for drug development. *Oncogene*, **19**: 6632–6641.

Bhattacharyya, D., Singh, S., Satnalika, N., Khandelwal, A. and Jeon, S. (2009) Nanotechnology, big things from a tiny world: A review. *International Journal of U and E Service, Science and Technology*, **2**: 29-38.

Bhatt, A., Mathur, R., Farooque, A., Verma, A. and Dwarakanath, B. (2010) Cancer biomarkers - current perspectives. *Indian Journal of Medical Research*, **2**: 129-149.

Bird, A.P. and Wolffe, A.P. (1999) Methylation-induced repression--belts, braces, and chromatin. *Cell*, **99**: 451-454.

Blackwood, E.M. and Eisenman, R.N. (1991) Max a helix-loop-helix zipper protein that forms a sequence-specific DNA-binding complex with Myc. *Science*, **251**: 1211-1217.

Bodemann, B.O. and White, M.A. (2013) Ras GTPases: Codon Bias holds Kras down but not out. *Current biology*, **23**: 70-75.

Bosse-Doenecke, E., Weininger, U., Gopalswamy, M., Balbach, J., Knudsen, S.M. and Rudolph, R. (2008) High yield production of recombinant native and modified peptides exemplified by ligands for G-protein coupled receptors. *Protein Expression and Purification*, **58**:114-121.

Bravo-codero, J.J., Hodson, L. and Condeelis, J. (2012) Directed cell invasion and migration during metastasis. *Current Opinion in Cell Biology*, **24**: 24277-24283.

Brenner, D.J. and Hall, E.J. (2007) Computed tomography-an increasing source of radiation exposure. *New English journal of medicine*, **3**: 2277-2284.

Budd, R. (2002) Death receptors couple to both cell proliferation and apoptosis. *Journal of Clinical Investigation*, **109**: 437-442.

Byrd, J.C. and Bresalier, R.S. (2004) Mucins and mucin binding proteins in colorectal cancer. *Cancer Metastasis Reviews*, **23**:77-99.

Carlo, M. and Croce, M.D. (2008) Oncogenes and cancer. *The New England Journal of Medicine*, **358**: 502-511.

Chang, Y., Yeh, K., Hsu, N.C., Lin, S., Chang, T. and Chang, J. (2010) Detection of N-, H- and Kras codons 12, 13 and 61 mutations with universal Ras primer multiplex PCR and N-,H-, and Kras specific primer extension. *Clinical Biochemistry*, **43**: 296-301.

Chen, X., Ko, L., Jayaraman, L. and Prives, C. (1996) P53 Levels, functional domains, and DNA damage determine the extent of the apoptotic response of tumor cells. *Genes and Development*, **10**: 2438-2451.

Chial, H. (2008) Proto-oncogenes to oncogenes to cancer. *Nature education*, **1**:1.

Choi, Y., Kwak, J. and Park, J. (2010) Nanotechnology for cancer detection. *Sensors*, **10**: 428-455.

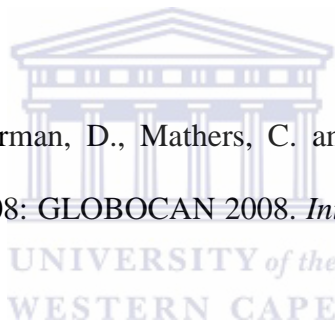
Citri, A., Alroy, I., Lavi, S., Rubin, C., Xu, W., Grammatikakis, N., Patterson, C., Neckers, L., Fry, D. and Yarden, Y. (2002) Drug-induced ubiquitylation and degradation of erbb receptor tyrosine kinases: Implications for cancer therapy. *The EMBO Journal*, **21**: 2407-2417.

Cordaux, R. and Batzer, M.A. (2009) The impact of retrotransposons on human genome evolution. *Nature review genetics*, **10**: 691-703.

Deaton, A. and Bird, A. (2011) CpG islands and the regulation of transcription. *Genes development*, **25**: 1010-1022.

Fearon, E. R. and Vogelstein, B. (1990) A genetic model for colorectal tumorigenesis. *Cell*, **61**:759-767.

Ferlay, J., Shin, H., Bray, F., Forman, D., Mathers, C. and Parkin, M. (2010) Estimates of worldwide burden of cancer in 2008: GLOBOCAN 2008. *International Journal of Cancer*, **127**: 2897 – 2917.



Feynman, R.P. (1960) There's Plenty of Room at the Bottom. *Engineering and Science*, **23**: 22-36.

Friesen, C., Herr, I., Krammer, P.H and Debatin, K.M. (1996) Involvement of the CD95 (APO-1/Fas) receptor/ligand system in drug-induced apoptosis in leukemia cells. *Nature Medicine*, **2**: 574-577.

Fu, A. Gu, W. Larabell, C. and Alivisatos, P. (2005) Semiconductor nanocrystals for biological imaging. *Current Opinion in Neurobiology*, **15**: 568-575.

Fujimura, J. (1988) The molecular biological bandwagon in cancer research: where social worlds meet. *Social Problems*, **35**: 261-283.

- Fulda, S. and Debatin, K.M. (2004) Exploiting the death receptor pathways for tumour therapy. *Biochemica et Biophysica*, **1705**: 27-41.
- Gao, X., Yang, L., Petros J., Marshall, F., Simons, J. and Nie, S. (2005). In Vivo Molecular Cellular Imaging with Quantum Dots. *Current Opinion in Biotechnology*, **16**: 63-72.
- Godefroy, N., Lemaire, C., Mignotte, B. and Vayssiere, J. (2006). P53 and Retinoblastoma Protein (Prb): A Complex Network of Interactions. *Apoptosis*, **11**: 659–661.
- Goodsell, D. (1999). The Molecular Perspective: The Ras Oncogene. *The Oncologist*, **4**: 263-264.
- Gottesman, S., Wickner, S. And Maurizi, M. (1997) Protein Quality control: Triage by chaperones and proteases. *Genes and Development*, **11**: 815-823.
- Grimminger, P.P., Maus, M.K., Schneider, P.M., Metzger, R., Hölscher, A.H., Sugita, H., Danenberg, P.V., Alakus, H. and Brabender, J. (2012) Glutathione S-transferase PI (GST-PI) mRNA expression and DNA methylation is involved in the pathogenesis and prognosis of NSCLC. *Lung Cancer*, **78**:87-91.
- Guo, W., Chen, N., Tu, Y., Dong, C., Zhang, B., Hu, C. and Chang, J. (2013) Synthesis of Zn-Cu-In-S/Zns core/shell quantum dots with inhibited blue-shift photoluminescence and applications for tumor targeted bioimaging. *Theranostics*, **3**: 99-108.
- Guz, A. and Ruchchitskii, Y. (2003). Nanomaterials; On the Mechanics of Nanomaterials. *International Applied Mechanics*, **39**: 1271-1293.
- Haglund, E.M., Seale-Goldsmith, M., Dhawan, D., Stewart, J., Ramos-Vara, J., Cooper, C.L., Reece, L.M., Husk, T., Bergstrom, D., Knapp, D., and Leary, J.F. (2008) Peptide targeting of quantum dots to human breast cancer cells. *Proceedings of SPIE*, **6866**: 68660S-1.

Hanahan, D. and Weinberg, R.A. (2000) The hallmarks of cancer. *Cell*, **100**: 57–70.

Harrington, J. (2007) Biology of cancer. *Medicine*, **36**: 689-692.

Hassan, S.E., Bekarev, M., Kim, M.Y., Lin, J., Piperdi, S., Gorlick, R. and Geller, D.S. (2012) Cell surface receptor expression patterns in osteosarcoma. *Cancer*, **118**: 740-749.

He, X., Chen, T. and Zhu, J. (2011) Regulation and function of DNA methylation in plants and animals. *Cell Research*, **21**: 442-465.

Heldin, C.H. and Westermark, B. (1999) Mechanism of action and in vivo role of platelet derived growth factor. *Physiology Review*, **79**: 1283-1316.

Hermanson, T.G. (2008) Bioconjugation Techniques, Second edition, Academic press, Elsevier Amsterdam, pp. 494-495.

Iglesias-Garcia, J., Dominiques- Monoz, E., Luzano -leon, A., Abdulkader, I., Larino-Noia, J., Atanez, J., and Forteza, J. (2007) Impact of endoscopic ultra sound- guided fine needle biopsy for diagnosis of pancreatic masses. *World Journal of Gastroenterology*, **13**: 289-293.

Ikeguchi, M., Gomyo, Y., Tsujitani, S., Maeta, M. and Koibara, N. (2000) Combined analysis of p53 and retinoblastoma protein expressions in esophageal cancer. *Annual Thoracic Surgeons*, **70**: 913-917.

Jackson, A. M, Boutell J, Cooley. N, and He.M. (2003) Cell-free protein synthesis for proteomics. Briefings in functional. *Genomics and Proteomics*, **2**: 308-319.

Jemal, A., Brag, F., Center, M., Ferlay, J., Ward, E. and Forman, D. (2008) Global cancer statistics. *CA Cancer Journal for Clinicians*, **61**: 69-90.

Janknecht, R. (2004) On the road to immortality: htert up-regulation in cancer cells. *FEBS Letters*, **564**: 9-13.

Kandilogiannaki, M., Koutsoudakis, G., Zafiropoulos, A., Krambovitis, E. (2001) Expression of a recombinant human anti-MUC1 scFv fragment in protease-deficient Escherichia coli mutants. *International journal of molecular medicine*, **6**: 659-664.

Karasseva, N.G., Glinsky, V.V., Ning, X., Chen, N.X., Komatireddy, R. and Quinn, T.P. (2002) Identification and characterization of peptides that bind human ErbB-2 selected from a bacteriophage display library. *Journal of Protein Chemistry*, **21**: 287-296.

Keaton, A.M. (2007). "The cell cycle: principles of control" By David O Morgan. *Cell Division*, **2**, 27.

Kelland, L.B. (2005) Overcoming the immortality of tumour cells by telomere and telomerase based cancer therapeutics - current status and future prospects. *European Journal of Cancer*, **41**: 971-979.

Kim, J., Ebersole, T., Kovprina, N., Noskov, N.V., Ohzeki, J., Masumoto, H., Mravinac, B., Sullivan, B.A., Pavlicek, A., Dovat, S., Pack, S.D., Kwon, Y., Flanagan, P.T., Laukinov, D., Lobanenkov, V. and Larionov, V. (2009) Human gamma-satellite DNA maintains open chromatin structure and protects a transgene from epigenetic silencing. *Genome research*, **19**: 533-544.

Koskinen, P.J. and Alitalo, K. (1993) Role of Myc amplification and over-expression in cell growth, differentiation and death. *Seminars in Cancer Biology*, **4**: 3-12.

Kruglyak, E., Freeman, L.M. and Wadle, S. (1997) Detection of occult gastric carcinoma with Indium-111 labeled CYT-103 (Oncoscint) immunoscintigraphy. *Annals of Oncology*, **8**:301-302.

Lin, B., Li, Y. and Robertson, K.D. (2011) DNA methylation: Superior or subordinate in the epigenetic hierarchy. *Genes and Cancer*, **2**: 607-617.

Lin, C.Y., Loven, J., Rahl, P.B., Paranal, R.M., Burge, C.B., Brudner, J.E., Lee, T.I. and Young, R.A. (2012) Transcriptional amplification in tumor cells with elevated c-Myc. *Cell*, **151**: 56-67.

Liu X., Jakubowski, M. and Hunt, J. (2011) KRAS gene mutation in colorectal cancer is correlated with increased proliferation and spontaneous apoptosis. *American Journal of Clinical Pathology*, **135**: 245-252.

Manning, D. (2004). The risk of cancer from radiography. *Radiography*, **10**: 171-172.

Martinez, J., Parker, M., Fultz, K., Ignatenko, N. and Gerner, E. (2003) Molecular biology of cancer. John Wiley&Sons, Inc.

Mayosi, B.M., Flisher, A., Lalloo, U.G., Sitas, F. and Brashaw, D. (2009) The burden of non-communicable diseases in South Africa. *Lancet*, **374**: 934- 947.

Metlitskaia, L., Cabralda, J.E., Suleman, D., Kerry, C., Brinkman, J., Bartfeld, D. and Guarna, M.M. (2004) Recombinant antimicrobial peptides efficiently produced using novel cloning and purification processes. *Biotechnology and Applied Biochemistry*, **39**: 339-345.

Mier, W., Kramer, S. Zitzmann, S., Altmann, A. Leotta, K., Schierbaum, U., Schnotzer, M., Eisenhut, M. and Haberkorn, U. (2013) PEGylation enables the specific tumor accumulation of a peptide identified by phage display. *Organic and Biomolecular Chemistry*, **11**: 2706-2711.

Mihara, M., Erster, S., Zaika, A., Petrenko, O., Chittenden, T., Pancoska, P. and Moll, U.M. (2003) p53 has a direct apoptogenic role at the mitochondria. *Molecular Cell*, **11**: 577-590.

Mishra, A. and Verma, M. (2010) Cancer biomarkers: Are we ready for prime time? *Cancers*, **2**: 190-208.

Montalbetti, C. and Falque, V. (2005) Amide bond formation and peptide coupling. *Tetrahedron*, **61**: 10827-10852.

Mousa, S.A. and Bharali, D. (2011) Nanotechnology-based detection and targeted therapy in cancer: nano-bio paradigms and applications. *Cancers*, **3**: 2888-2903.

Nakajima, N. and Ikada, Y. (1994) Mechanism of amide bond formation by carbodiimide for bioconjugation in aqueous media. *Bioconjugate Chemistry*, **6**:123-130.

Näthke, I. (2004) APC at a glance. *Journal of Cell Science*, **117**: 4873-4875.

National industrial chemical notifications and Assessment scheme. (2006) Nanomaterials, Department of Health and Ageing. Australia.

Neel, N.F., Rossman, K.L., Martin, T.D., Hayes, T.K., Yeh, J.J. and Der, C.J. (2012) The RalB small GTPase mediates formation of invadopodia through a GTPase-activating protein-independent function of the RalBP1/RLIP76 effector. *Molecular and Cellular Biology*, **32**: 1374-86.

Noel, T. Sals, T. and Lillie, S. (2007) Systemic review: The long term effects of false positive mammograms. *Annals of International Medicine*, **502**: 146-147.

Novagen. (2003) pET system manual, 10th edition, Darmstadt, Germany.

Novagen. (2001) Protein expression Novagen catalogue, Darmstadt, Germany.

Novakofski, J. (1991) Role of proto-oncogenes in normal growth and development. *Journal of Animal Science*, **69**: 56-73.

Ozoren, N. and El-Derry, W.S. (2003) Cell surface death receptor signaling in normal and cancer cells. *Seminars in Cancer Biology*, **13**:135-147.

Pattabiraman, V.R and Bode, J.W. (2011) Rethinking amide bond synthesis. *Nature*, **480**: 471-479.

Rabeneck, L., Zwaal, C., Goodman, J.H., Mac, V. and Zamkanei, M. (2008) Cancer care ontario guaiac faecal occult blood test (Fobt) laboratory standards. Evidentiary base and recommendations. *Clinical Biochemistry*, **41**: 1289-1305.

Rasmussen, U.B., Schreiber, V., Schultz, H., Mischler, F. and Schughart, K. (2002) Tumor cell-targeting by phage-displayed peptides. *Cancer Gene Therapy*, **9**: 606-612.

Research Advocacy Agency Network (2010). Biomarkers in Cancer. An Introductory Guide For Advocates.

Reubi, J.C. (2003) Peptide Receptors as Molecular Targets for Cancer Diagnosis and Therapy. *Endocrine Reviews*, **24**: 389–427.

Roth, W., Stenner-Liewen, F., Pawlowski, K., Godzik, A. and Reed, J.C. (2001) Identification and characterization of DEDD2, a death effector domain-containing protein. *Journal of Biology and Chemistry*, **277**: 7501-7508.

Sarbeni, S., Rondonotti, E., Iozzelli, A., Spinal, G.E., Cavallaro, F., Ciscato, C., De-franchis, R., Sardanell, F. and Vecchi, M.(2007) Imaging of the small bowel in crohn's disease: A review of old and new techniques. *Old of Gastroenterology*, **13**: 3279-3287.

- Satakarni, M .and Curtis, R. (2011) Production of recombinant peptides as fusions with SUMO. *Protein expression and purification*, **78**: 113-119.
- Schmidt, C. (2007). Book review of "The molecular biology of cancer". *Molecular Cancer*, **6**: 72.
- Shadidi, M. and Sioud, M. (2002). Identification of novel carrier peptides for the specific delivery of therapeutic into cancer cells. *FASEB*.
- Shadidi, M. and Sioud, M. (2003). Selective targeting of cancer cells using synthetic peptides. *Drug resistance updates*, **6**: 363–371.
- Shaw, A., Winslow, M.M., Magendantz, M., Ougang, C., Dowdle, J., Subramanian, A., Lewis, T., Maglathin, R.L., Tolliday, N. and Jacks, T. (2011) Selective killing of K-ras mutant cancer cells by small molecule inducers of oxidative stress. *PNAS*, **21**: 8773–8778.
- Singhal, S., Vachani, A., Antin-Ozerkis, D., Kaiser, L. and Albelda, S. (2005) Prognostic implications of cell cycle, apoptosis and angiogenesis biomarkers in small- cell lung cancer: A Review. *Clinical Cancer Research*, **11**: 3974-3986.
- Smith, A.M., Gao, X. and Nie, S. (2004) Quantum dot nanocrystals for in vivo molecular and cellular imaging. *Photochemistry and Photobiology*, **80**: 000-000.
- Smith, A.M. and Nie, S. (2004) Chemical analysis and cellular imaging with quantum dots. *The Analyst*, **129**: 672-677.
- Smith, G., Carey, A.F., Beattie, J., Wikie, M.J.V., Lightfoot, T.J., Coxhead, J., Gamer R.C., Steele, R.J.C., and Wolf C.R. (2002) Mutations in APC, Kirsten-ras, and p53—alternative genetic pathways to colorectal cancer. *PNAS*, **14**: 9433–9438.

St. Croix, B., Rago, C., Velculescu, V., Traverso, G., Romans, K., Montgomery, E., Lal, A., Riggins, G., Lengauer, C., Vogelstein, B. and Kinzler, K. (2000) Genes Expressed in Human Tumor Endothelium. *Science*, **289**: 1197 -1202.

Strathdee, G. and Brown, R. (2002) Aberrant DNA methylation in cancer; potential clinical interventions. Cambridge University press, pp. 1-17.

Uhlén, M. and Abrahamssén, L. (1989) Secretion of recombinant proteins into the culture medium by *Escherichia coli* and *Staphylococcus aureus*. *Biochemical Society Transactions*, **17**:340-341.

Urbanelli, L., Ronchini, C., Fontana, L., Menard, S., Orlandi, R. and Monaci, P. (2001) Targeted gene transduction of mammalian cells expressing the HER2/neu receptor by filamentous phage. *Journal of Molecular Biology*, **313**: 965-976.

Valeur, E. and Bradley, M. (2009) Amide bond synthesis beyond the myth of coupling reagents. *Chemical society reviews*, **38**: 606-631.

Vert, M., Doi, Y., Hellwich, K., Hess, M., Hodge, P., Kubisa, P., Rinaudo, M., and Schué, F. (2012) Terminology for biorelated polymers and applications (IUPAC Recommendations 2012). *Pure Applied Chemistry*, **84**: 377–410.

Vojtek, A. B. and Der, C. J. (1998) Increasing complexity of the Ras signaling pathway. *Journal of Biological Chemistry*, **273**: 19925-19928.

Wang, X., Yang, L., Chen, Z. and Shen, D. (2008). Application of nanotechnology in cancer therapy and imaging. *CA, A Cancer Journal for Clinicians*, **58**: 97-110.

Williams, A., and Ibrahim, I. T. (1981). Carbodiimide Chemistry: Recent Advances. *Chemical Reviews*, **81**:589-636.

Wu, P., Leinonen, J., Koivunen, E., Lankinen, H. and Stenman, U.H. (2000) Identification of novel prostate-specific antigen-binding peptides modulating its enzyme activity. *European Journal of Biochemistry*, **267**:6212–6220.

WHO (2008) World Cancer Report 2008, Lyon: International Agency for Research on Cancer.

Young, K., Xie, Q., Zhou, G., Eichhoff, J., Sanger, W.G. Aoun, P. and Chan, W.C. (2008) Transformation of follicular lymphoma to precursor b-cell lymphoblastic lymphoma with c- myc gene rearrangement as a critical event. *American Journal Clinical Pathology*, **129**:157-166.

Young, A., Lou, D. and McCormick, F. (2013) Oncogenic and Wild-type Ras Play Divergent Roles in the Regulation of Mitogen-Activated Protein Kinase Signaling. *Cancer Discovery*, **3**:112-123.

Yu, D. and Hung, M. (2000) Overexpression of ErbB2 in cancer and ErbB2-targetting strategies. *Oncogene*, **53**: 6115-6121.

Zhang, W., Zhang, C., Zhang, L. and Liu, S. (2008) Occurrence of cancer at multiple sites: Towards distinguishing multigenesis from metastasis. *Biology Direct*, **3**:14.

Zhao, M., Sun, J. and Zhao, Z. (2012) Distinct and competitive regulatory patterns of tumor suppressor genes and oncogenes in ovarian cancer. *Plos*, **7**: 1-13.

Zornig, M., Hueber, A., Baum, W. and Evan, G. (2001) Apoptosis regulators and their role in tumorigenesis. *Boichemica et Biophysica*, **1551**: F1-F37.

Zhou, M. and Ghosh, I. (2006) Quantum dots and peptides: a bright future together. *Current Trends in Peptide Science*, **88**: 325-339.



UNIVERSITY *of the*
WESTERN CAPE